(room temperature, 30 minutes) and imaged with 3,3′,5,5′-tetramethylbenzidine (TMB) substrate solution (50 μL; T4444; Sigma-Aldrich) followed by addition of 1 N H_2SO_4 and read at 450 nm wavelength with Benchmark ELISA plate reader (Bio-Rad Laboratories, Hercules, CA). The accuracy and precision of the assay were determined (Table S1, available on the *Blood* website; see the Supplemental Materials link at the top of the online article).

Free GM-CSF. Serum concentrations of free GM-CSF (ie, not bound to GM-CSF autoantibody) were measured using Quantikine HS Human GM-CSF ELISA kits (R&D Systems) according to the manufacturer's instructions. The sensitivity of the assay was 0.26 pg/mL.

Total GM-CSF. Serum concentrations of total GM-CSF (ie, autoantibody-bound plus free GM-CSF) were measured using a novel sandwich ELISA based on a method developed for measurement of HIV-1 p24 antigen.[35] Microtiter plates were coated with capture antibody (PBS containing 1 μg/mL rabbit anti–human GM-CSF antibody, 4°C, overnight), and blocked with PBS containing 1% (wt/vol) BSA. To evaluate the detection of free GM-CSF and autoantibody-bound GM-CSF in serum, a set of standard samples composed of recombinant human GM-CSF (Leukine) ranging from 0 to 30 ng/mL was prepared in mouse serum in the absence or presence of purified human GM-CSF autoantibodies (30 μg/mL). Aliquots (10 μL) of serum or standard control samples were mixed with 20 μL pretreatment buffer (SDS-HD buffer; PBS, 1% SDS, 1.5 mM diethylenetriamine pentaacetic acid, pH 7.4, and incubated (95°C, 5 minutes). After chilling briefly on ice, 270 μL PBS containing 1% (wt/vol) BSA was added to quench residual SDS. Duplicate aliquots (50 μL) of samples were applied to wells, and the plates were incubated (room temperature, 90 minutes), washed, and then incubated with detection antibody solution (PBS containing 1% [wt/vol] BSA, 500 ng/mL biotin-conjugated goat anti–human GM-CSF antibody; room temperature, 90 minutes). Detection was enhanced by incubation with ExtrAvidin HRP solution (diluted 1/250; room temperature, 30 minutes), imaged by TMB solution followed by addition of 1 N H_2SO_4 and read at a wavelength of 450 nm with Benchmark ELISA plate reader.

Phospho-STAT5 immunoblotting

Neutrophils were isolated on Ficoll gradients, followed by red blood cell lysis. More than 97% of the isolated cells consist of granulocytes. Isolated neutrophils were resuspended (5×10^6 cells/mL) in assay buffer (Hank balanced salt solution [HBSS] containing 10% fetal bovine serum, 25 mmol/L HEPES, pH 7.4) and incubated with various concentrations of purified GM-CSF autoantibodies (0, 0.01, 0.1, 0.5, 1.0 μg/mL) and GM-CSF (Leukine, 10 ng/mL) for 15 minutes at 37°C. After incubation, cells were collected by centrifugation, washed with PBS, and suspended in 200 μL RIPA buffer, which consisted of 0.05 mol/L Tris-HCl, pH 8.0, 0.15 M NaCl (Tris-buffered saline [TBS]), 1% [vol/vol] Nonidet P-40, 0.5% [wt/vol] sodium deoxycholate, 0.1% [wt/vol] SDS, 0.004% [wt/vol] sodium azide) containing 2% (vol/vol) proteinase inhibitor cocktail, phenylmethylsulfonyl fluoride, and sodium orthovanadate as directed by the manufacturer. Samples were kept on ice for 30 minutes, and soluble lysate was collected after removing insoluble debris (9000*g*, 4°C, 15 minutes). Neutrophil lysate was then fractionated on SDS-PAGE gels (4%-12% Tris Glycine Gel; Invitrogen) and transferred to PVDF membranes by electroblotting. After blocking the membrane with TBS, 5% [wt/vol] dry milk, 0.1% [vol/vol] Tween 20 (4°C, overnight), phosphorylated-STAT5 was detected with murine anti–phospho-STAT5 antibody (diluted 1/500) followed by the incubation with HRP-conjugated sheep anti–murine IgG and imaged with ECL-Plus (GE Healthcare) as directed by the manufacturer. This procedure was used for measuring STAT5A, STAT5B, total STAT5, and actin in the same samples with the appropriate antibodies. Band intensity was quantified using KODAK Image Station 440FC equipped with KODAK 1D Image Analysis Software (Carestream Health, Rochester, NY), and the ratio of phosphorylated STAT5 to total STAT5 was calculated.

Serum GM-CSF–neutralizing capacity (TF-1 cell) assay

GM-CSF neutralization activity was evaluated using the GM-CSF–dependent cell line, TF-1 as described previously.[20] In brief, cells were cultured in the absence or presence of GM-CSF autoantibodies purified from equal volumes (30 μL) of serum or IVIG (600 μg/well). After 4 days in culture, cell proliferation was measured using the TACS 3-(4,5-dimethylthiazol-2-yl)-2,5-diphenyltetrazolium assay kit (R&D Systems) according to the manufacturer's instructions.

Neutrophil CD11b stimulation index assay

The neutrophil stimulation assay was performed as described previously.[5] In brief, aliquots of heparinized fresh whole blood were incubated with GM-CSF, and then cell-surface CD11b levels were quantified by flow cytometry. The CD11b stimulation index is calculated as the mean fluorescent intensity of stimulated neutrophils minus the mean fluorescent intensity of unstimulated neutrophils divided by mean fluorescent intensity of unstimulated neutrophils and multiplied by 100.

Neutrophil chemotaxis assay

Neutrophils were isolated as above and suspended (4×10^6 cells/mL) in HBSS supplemented with 0.1% (wt/vol) BSA, 1 mM $CaCl_2$, and 1 mM $MgCl_2$ with or without various doses of GM-CSF autoantibodies. Neutrophil chemotactic capacity was evaluated using Transwell (Corning Life Sciences, Acton, MA) with 3-μm pore size with 10 ng/mL rhIL-8 as a chemoattractant. One hundred microliters of cell suspension was transferred to upper chamber and incubated for 2 hours at 37°C, 5% CO_2. After incubation, neutrophils migrating into the lower chamber were enumerated using a hemocytometer.

Neutrophil phagocytosis assay

The phagocytic capacity of neutrophils in whole blood (hereafter called the phagocytic capacity) was measured by flow cytometry as described previously.[5] In brief, triplicate samples of heparinized human blood were incubated with IgG-opsonized fluorescent microspheres[32] with gentle orbital rotation. Uptake of microspheres by neutrophils was evaluated with flow cytometry. Phagocytic capacity was calculated as the percentage of neutrophils containing internalized microspheres multiplied by the mean fluorescence intensity of phagocytic neutrophils and multiplied by the neutrophil count in blood. This assay was validated using isolated neutrophils (Figure S2).

Alveolar macrophage phagocytosis assay

Human alveolar macrophages were obtained from lung bronchoalveolar or whole lung lavage fluid and then washed, resuspended, and seeded into 35-mm culture dishes as described previously.[1] Cells were incubated with heat-killed *E coli*, *Staphylococcus aureus*, zymosan, or 0.1-μm latex beads, each fluorescently labeled with Texas Red (Invitrogen), fixed and examined by fluorescence microscopy[36] as described previously[1] to evaluate alveolar macrophage phagocytosis.

Statistical analysis

Numerical data were evaluated for a normal distribution using the Kolmogorov-Smirnov test and for equal variance using the Levene median test; parametric data are presented as means (± SE), and nonparametric data are presented as medians and interquartile ranges. Categorical data are presented as a percentage of the total or numerically, as appropriate. Statistical comparisons of parametric data were made with the Student *t* test for 2-group comparisons and with Kruskal-Wallis one-way analysis of variance with post-hoc analysis according to the Holm-Sidak method for multiple-group comparisons. Nonparametric data were compared with the use of the Kruskal-Wallis rank-sum test. Correlation coefficients were obtained using the Spearman correlation method. All tests were 2-sided, and *P* values of less than .05 were considered to indicate statistical significance. Regression analysis was performed with Spearman rank order correlation

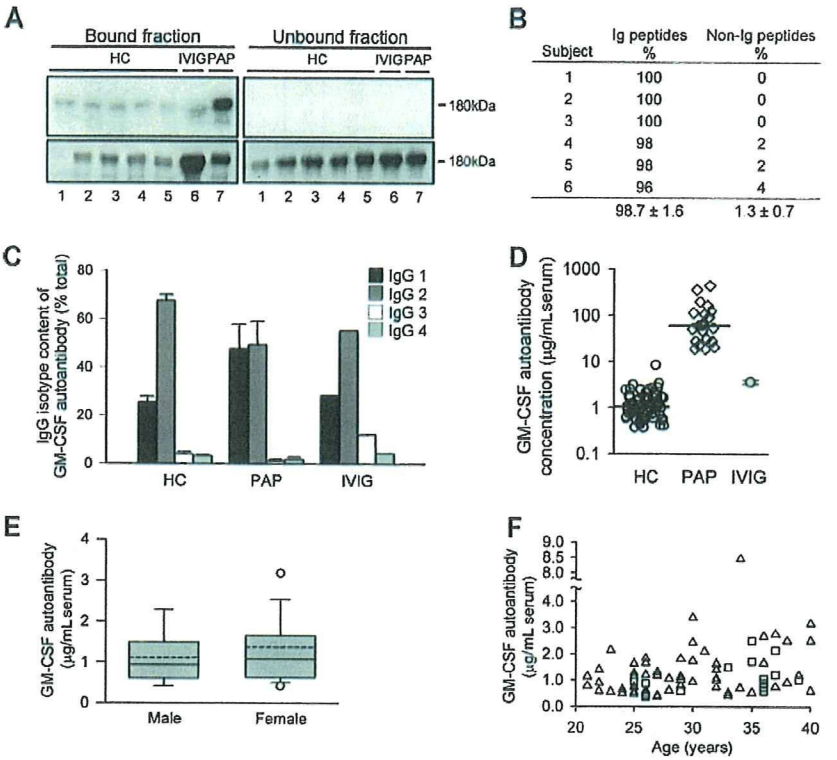

Figure 1. Presence of GM-CSF autoantibodies in healthy subjects. (A) Total IgG was isolated from the serum of healthy control subjects (HC) or patients with PAP (PAP) or from pharmaceutical grade IVIG by protein G chromatography and subjected to ultrafiltration under acidic conditions to remove bound GM-CSF. GM-CSF autoantibodies were then isolated by GM-CSF affinity chromatography and evaluated by far-Western analysis probed with ^{125}I-GM-CSF. Shown are Coomassie Blue–stained electrophoresis gels (bottom panels) and corresponding far-Western blots (top panels). Each numbered lane represents the corresponding bound (left panels) and unbound (right panels) chromatography fractions from 1 subject or sample. (B) Serum GM-CSF–binding proteins from 6 healthy human subjects were fractionated individually on gels as in panel A, and proteins in the 180-kDa band from each were extracted, subjected to liquid chromatography and tandem mass spectroscopy, and the results evaluated by comparison to Mascot database as described under "Methods." Only matches with a probability-based Mowse score greater than 64 (indicating a P value $< .05$) were considered in the analysis. The percentages of immunoglobulin (Ig) and non-Ig peptides among the top 50 peptide fragment matches identified for each sample are shown. (C) GM-CSF autoantibodies were isolated by GM-CSF affinity chromatography from serum of healthy subjects (HC; n = 10), patients with PAP (PAP, n = 4), or from pharmaceutical IVIG (n = 1 clinical grade vial), and the percentage of IgG subtypes was measured by ELISA. (D) Serum GM-CSF autoantibody concentrations in healthy subjects (HC), patients with PAP (PAP), or IVIG (reconstituted at 9.94 mg/mL in PBS). Serum GM-CSF autoantibody levels in healthy subjects (median (interquartile range [IQR]) = 1.04 [0.63-1.7] μg/mL, n = 72) were lower than in patients with PAP (median [IQR] = 59.8 (27.4–116.5) μg/mL; n = 21; $P < .001$). Median values (HC, PAP) are indicated by a horizontal bar. (E) Serum GM-CSF autoantibody levels in males (n = 15) and females (n = 57). Data are shown as whisker plots indicating the interquartile range (upper and lower borders of box), the 90th and 10th percentile (error bars), the 95th and 5th percentile (upper and lower open symbols), the median (solid horizontal line in box), and mean (dashed line in box) values of GM-CSF autoantibody levels. (F) Serum GM-CSF autoantibody levels in healthy women (△) and men (□) of various ages (n = 72). Regression analysis did not reveal a significant correlation GM-CSF autoantibody levels with age ($R^2 = 0.08$).

using SigmaPlot software (version 8.0; Systat Software, San Jose, CA). All experiments were repeated at least twice, with similar results.

Results

Circulating GM-CSF autoantibodies in healthy subjects

To determine whether GM-CSF autoantibodies are normally present in healthy persons, we used a novel method[29] based on the prior removal of potentially bound GM-CSF. GM-CSF-binding immunoglobulins similar in molecular weight to IgG were detected in all healthy subjects evaluated, in pharmaceutical IVIG, and in a patient with PAP (as a positive control; Figure 1A). Liquid chromatography and tandem mass spectroscopy confirmed the authenticity of the autoantibodies in healthy subjects, demonstrating they were composed exclusively of immunoglobulin (Figure 1B). IgG subtyping further demonstrated they were composed primarily of IgG1 and IgG2 with only small amounts of IgG3 and IgG4 and had a similar composition in healthy persons, patients with PAP, and IVIG (Figure 1C). Using a sensitive and specific ELISA (Figure S1A-C), GM-CSF autoantibodies were detected in all samples evaluated, including the serum from 72 healthy persons, 21 patients with PAP, and IVIG (Figure 1D). The serum concentration of GM-CSF autoantibodies in healthy subjects was similar to that of pharmaceutical IVIG reconstituted at physiologic serum IgG concentration and was markedly lower than serum levels in patients with PAP (Figure 1D). GM-CSF autoantibody levels in healthy subjects were unaffected by sex (Figure 1E) or age (Figure 1F). These results demonstrate that GM-CSF autoantibodies are common or ubiquitous in healthy persons, albeit at levels far lower than in patients with PAP.

Circulating complexes of autoantibody and GM-CSF

To determine whether GM-CSF was bound to circulating GM-CSF autoantibodies, potentially interfering with detection, total serum IgG was isolated on protein G, washed to remove proteins not directly bound to autoantibodies, eluted, and evaluated by Western blotting. GM-CSF bound to IgG was present in all healthy subjects and in patients with PAP evaluated, thus demonstrating the presence of GM-CSF-autoantibody complexes (Figure 2A). To determine whether immune complex formation interfered with detection of serum GM-CSF, we first measured the concentration of GM-CSF in the absence or presence of GM-CSF autoantibodies. GM-CSF autoantibodies completely abolished detection of GM-CSF using a commercially available ELISA

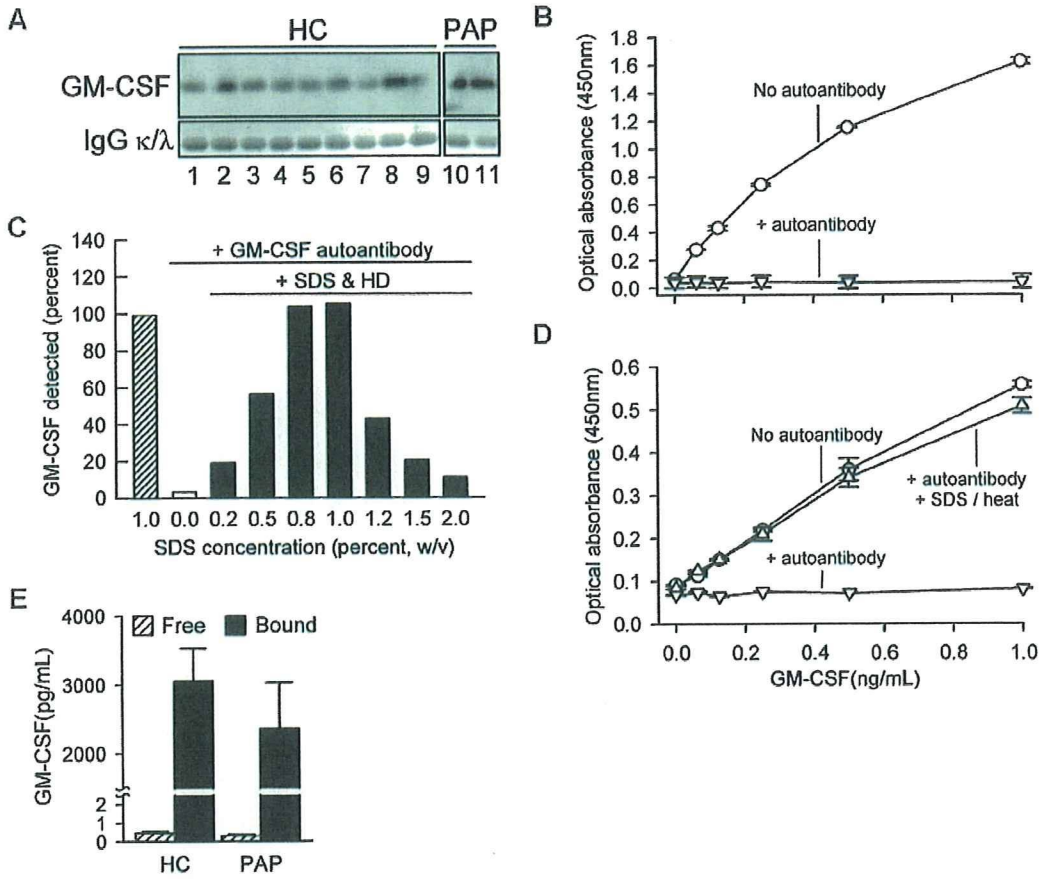

Figure 2. Concentration of free and IgG-bound GM-CSF in human serum. (A) Total IgG was isolated individually from the sera of healthy subjects (HC) or patients with PAP (PAP) using protein G and evaluated by Western blotting to detect GM-CSF (top panels) or IgGκ (κ) and -λ (λ) light chains (as a loading control, bottom blots). Each lane represents one subject. (B) Detection of free GM-CSF and autoantibody-bound GM-CSF in serum. A set of "standard" samples composed of recombinant human GM-CSF (Leukine) at various concentrations ranging from 0 to 30 ng/mL were prepared in mouse serum in the absence (○) or presence (▽) of purified human GM-CSF autoantibodies (30 μg/mL). Standard samples were diluted 1/30 with 1% BSA in PBS and then GM-CSF was measured using a commercial human ELISA kit (R&D Systems) as directed by the manufacturer. (C) Use of a novel ELISA (SDS-HD ELISA, see "Methods") to quantify GM-CSF in PBS in the absence or presence of GM-CSF autoantibody (1 μg/mL) and in the absence or presence of a pretreatment with SDS and heat denaturation. Each bar represents the mean of duplicate determinations for 1 of 4 separate experiments with similar results. (D) GM-CSF level evaluated using a novel human GM-CSF ELISA as described in "Methods." Symbols represent the same samples and conditions as described in the legend to panel B above. GM-CSF was detectable in the absence of GM-CSF autoantibody (○), undetectable in the presence of GM-CSF autoantibody in the absence of SDS-HD pretreatment (▽), and detection was restored in the presence of GM-CSF autoantibody by SDS-HD pretreatment (△). (E) Free GM-CSF (▨) or total GM-CSF (free and autoantibody-bound; ■) were measured in sera of healthy subjects (HC) or patients with PAP (PAP) using a commercially available ELISA or the SDS-HD ELISA, respectively, as described in "Methods." Total serum GM-CSF levels in HC and PAP were not different (3048 ± 484, n = 11; PAP 2360 ± 668, n = 5; respectively, $P = .43$).

(Figure 2B). We then developed a novel ELISA using a polyclonal capture antibody and pretreatment with SDS and heat denaturation that enabled detection of both free GM-CSF and GM-CSF bound to autoantibody (Figure 2C,D). Using this ELISA, the mean (± SE) total serum GM-CSF concentration in healthy subjects was 3047 plus or minus 484 pg/mL (Figure 2E). Similar levels of total serum GM-CSF levels were observed in patients with PAP. In contrast, levels of free GM-CSF measured using the commercial ELISA (see Figure 2B) were less than 1 pg/mL in both groups (Figure 2E). Thus, serum GM-CSF was more abundant than previously reported[12,13] and existed almost exclusively in a form complexed to IgG in health and disease with less than 0.1% present in the unbound form.

Effects of circulating GM-CSF autoantibodies on GM-CSF signaling

To determine the significance of GM-CSF autoantibodies in healthy subjects, we evaluated their effects on GM-CSF signaling. Using a bioassay based on GM-CSF–dependent proliferation of TF-1 cells,[20] autoantibody-dependent GM-CSF–neutralizing activity was detected in IgG isolated from all persons evaluated, and levels fell between that of serum from a patient with PAP as a positive control and culture media as a negative control (Figure 3A). IVIG reconstituted at physiologic IgG concentration also contained GM-CSF–neutralizing activity at levels similar to serum from healthy subjects. GM-CSF autoantibodies reduced GM-CSF signaling in a concentration-dependent fashion as shown by the decrease in GM-CSF–stimulated phosphorylation of signal transducer activation and transcription 5 (STAT5), a downstream signaling molecule (Figure 3B). Although low concentrations of free GM-CSF were highly bioactive, 5-fold higher concentrations of autoantibody-bound GM-CSF had practically no signaling activity (Figure 3C). GM-CSF stimulates increased levels of CD11b on neutrophils, a phenomenon we previously exploited in developing an assay to measure GM-CSF–neutralizing activity in whole blood.[5] Low concentrations of GM-CSF–stimulated maximal CD11b levels in healthy persons but had no effect in patients with PAP (Figure 3D). The block in stimulation of CD11b levels caused by higher GM-CSF autoantibody levels in patients with PAP could be overcome by exposure to high concentrations of GM-CSF (Figure 3D inset). Highly purified GM-CSF autoantibodies

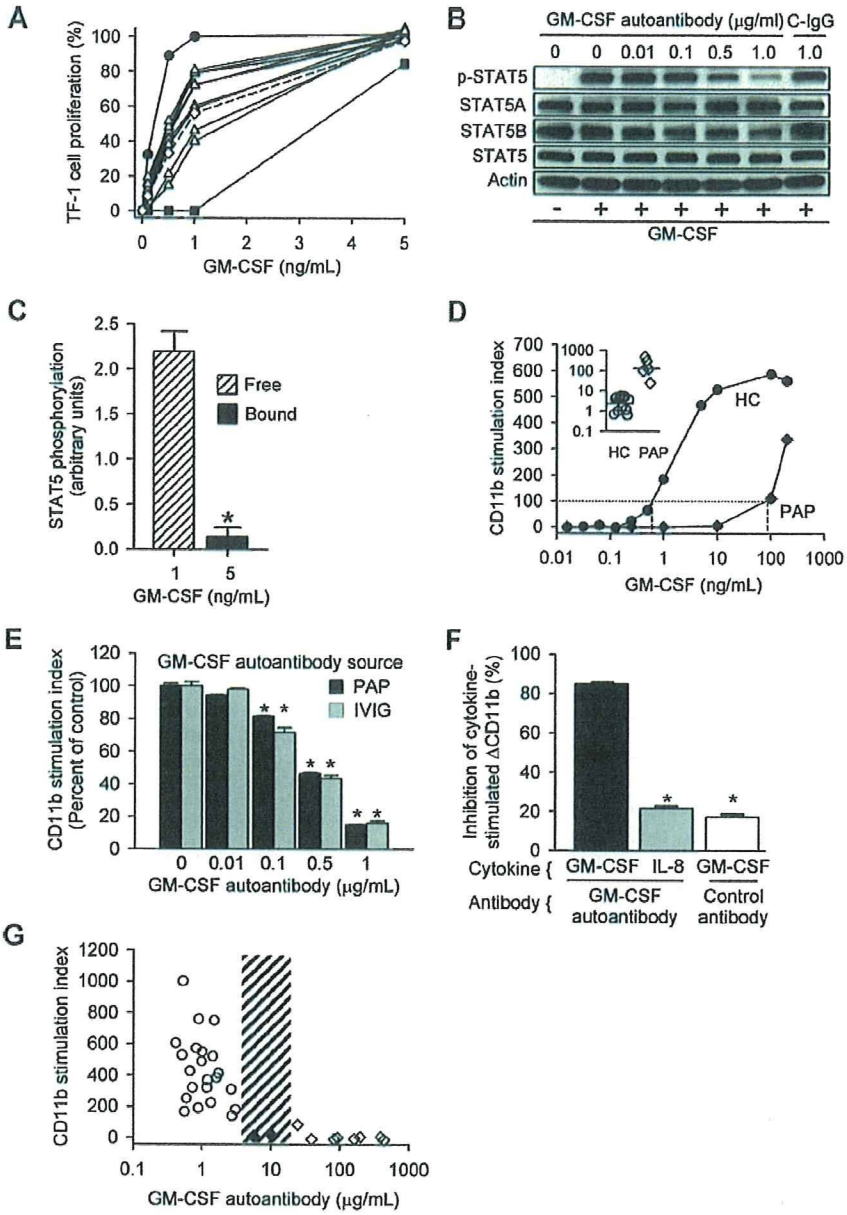

Figure 3. Regulation of GM-CSF signaling by GM-CSF autoantibodies in healthy subjects and patients with PAP. (A) The serum GM-CSF–neutralizing capacity of GM-CSF autoantibodies was measured using the TF-1 cell-proliferation assay.[20] Equal volumes (30 μL) of serum from healthy subjects (△) or a PAP patient (■) (as a positive control), IVIG reconstituted at physiologic concentration (◇), or culture media (●) (as a negative control) were evaluated. The neutralizing capacity of purified GM-CSF autoantibodies from HC serum or IVIG (dashed line) was intermediate between that of autoantibodies isolated from serum the patient with PAP, which contains high concentrations of GM-CSF autoantibody, and control media, which contains none. (B) Neutrophils isolated from healthy subjects were incubated with various concentrations of GM-CSF affinity-purified autoantibodies isolated from IVIG or with control antibody (1 μg/mL) and stimulated with 10 ng/mL GM-CSF for 15 minutes and total and phosphorylated STAT5 (pSTAT5) was measured by immunoblotting. (C) The signaling activity of free and autoantibody-bound GM-CSF was measured by quantifying the level of STAT5 phosphorylation in isolated neutrophils by immunoblotting (shown as the ratio of phosphorylated STAT5 to total STAT5) as described in "Methods." The signaling activity of GM-CSF complexed to autoantibody was markedly lower than free GM-CSF (0.142 ± 0.1 vs 2.192 ± 0.2 pg/mL, respectively; n = 3 each; $^*P < .001$). (D) The typical pattern of GM-CSF–stimulated increase in CD11b levels on neutrophils in whole blood (CD11b stimulation index) is shown for a healthy subject (HC) and a patient with PAP (PAP). The amount of exogenous GM-CSF (dashed lines) required to stimulate an increase in neutrophil CD11b levels to the threshold value (dotted line) was lower in HCs than in patients with PAP. The median (IQR) GM-CSF concentration required to reach this stimulation threshold (inset) was significantly higher in patients with PAP than in healthy subjects (120 [80-347] ng/mL, n = 5; and 3.96 [1.07-4.86] ng/mL; n = 12; respectively; $P < .002$, Mann-Whitney). (E) Concentration-dependent reduction in the CD11b stimulation index by GM-CSF autoantibody purified from IVIG (□) or patients with PAP (■) and incubated with fresh whole blood at various concentrations. Each bar represents the results of 3 separate determinations. *Significant decrease ($P < .001$) from baseline determined in the absence of GM-CSF autoantibody. (F) Specificity of purified GM-CSF autoantibody. Neutrophils were incubated in the presence of GM-CSF (10 ng/mL) or IL-8 (100 ng/mL) and in the absence or presence of 1 μg GM-CSF autoantibody or control IgG as indicated. Data represent the level of CD11b in stimulated cells—the level in unstimulated cells. GM-CSF autoantibodies markedly inhibited the GM-CSF–stimulated (■), but resulted in levels of inhibition by IL-8 (□) that were significantly lower and similar to control (IgG, □). *A significant difference ($P < .001$) compared with inhibition of the GM-CSF–stimulated increase by GM-CSF autoantibody (■). (G) The CD11b stimulation index was measured in fresh blood from healthy control subjects (○), patients with PAP with active disease (◇), or patients with PAP in clinical remission of the lung disease (♦). The range of serum GM-CSF autoantibody levels separating healthy subjects and patients with PAP with active disease evaluated with this assay is indicated (3.2-24 μg/mL, ▨). Each symbol represents the results of triplicate determinations for one subject. The median (IQR) free serum GM-CSF level in healthy subjects was 0.00 (0.00-0.390) pg/mL and did not correlate with the CD11b stimulation index ($P > .05$), whereas the median (IQR) GM-CSF autoantibody level (0.90 [0.58-1.19] μg/mL) correlated with CD11b stimulation index ($R^2 = 0.46$, $P = .03$) (Spearman rank order correlation).

isolated from IVIG or patients with PAP blocked the increase in CD11b levels to a similar degree and in a concentration-dependent fashion (Figure 3E). Purified GM-CSF autoantibodies were specific and did not block an IL-8–stimulated increase in CD11b levels (Figure 3F). To determine the endogenous autoantibody level associated with complete loss of GM-CSF signaling in vivo, the CD11b stimulation index was measured in whole blood from healthy subjects and patients with PAP. The CD11b stimulation index correlated inversely with endogenous levels of serum GM-CSF autoantibody up to 5.7 μg/mL and was zero over a wide range of higher concentrations (Figure 3G). It is noteworthy that all positive results below this autoantibody level (referred to as the critical threshold for CD11b stimulation) were from healthy subjects and all negative results above it were from patients with PAP. Thus, GM-CSF autoantibodies seem to scavenge free GM-CSF in vivo and modulate the endocrine signaling capacity of GM-CSF in whole blood, suggesting that they may function to negatively regulate GM-CSF signaling in health and disease.

Effects of circulating GM-CSF autoantibodies on myeloid cell functions

The functional significance of GM-CSF autoantibodies in healthy subjects was evaluated by correlating levels with endogenous neutrophil functions. We recently developed a method to measure neutrophil phagocytosis in whole blood and then showed that transfer of GM-CSF autoantibodies into healthy human blood reduced neutrophil phagocytosis in a concentration-dependent fashion.[5] Here, we verified that the assay can detect differences in the baseline phagocytic capacity of neutrophils among healthy subjects (Figure S2) and then measured the endogenous, phagocytic capacity of unstimulated neutrophils in whole blood from healthy subjects and patients with PAP. Neutrophil phagocytic capacity decreased with increasing endogenous GM-CSF autoantibody levels up to 3.2 μg/mL in healthy persons and reached a trough level and was unchanging over a wide range of higher concentrations above 39 μg/mL in patients with active PAP (Figure 4A). Two patients in remission of PAP lung disease who had lower serum GM-CSF autoantibody levels (5.7 and 10.4 μg/mL) had a neutrophil phagocytic capacity in the normal range, indicating the critical threshold of serum GM-CSF autoantibodies associated with reduced neutrophil phagocytosis might lie between 10.4 and 39 μg/mL. GM-CSF autoantibodies, at levels similar to those present in healthy subjects, reduced interleukin 8–stimulated neutrophil chemotaxis in vitro in a concentration-dependent fashion by a mechanism not attributable to chemokinesis or nonspecific effects (Figure 4B). Together, these results suggest that the low levels of GM-CSF autoantibodies present in healthy subjects may regulate GM-CSF–dependent neutrophil functions rheostatically and that the critical threshold level of GM-CSF autoantibodies associated with loss of GM-CSF priming of neutrophil functions in patients with PAP is between 10.4 and 39 μg/mL.

Because GM-CSF deficiency in mice impairs alveolar macrophage functions, including phagocytosis of *E coli*, *S aureus*, *Mycobacterium tuberculosis*, yeast particles (zymosan), and latex beads,[1,32,37,38] we evaluated phagocytic function of alveolar macrophages from healthy subjects and patients with autoimmune PAP. Compared with alveolar macrophages from healthy subjects, alveolar macrophages from patients with PAP had impaired phagocytosis of *E coli*, *S aureus*, zymosan, and latex beads (Figure S3) and impaired clearance of surfactant (not shown). Although high levels of GM-CSF autoantibodies are thought to cause lung disease in PAP by blocking the paracrine stimulation of alveolar

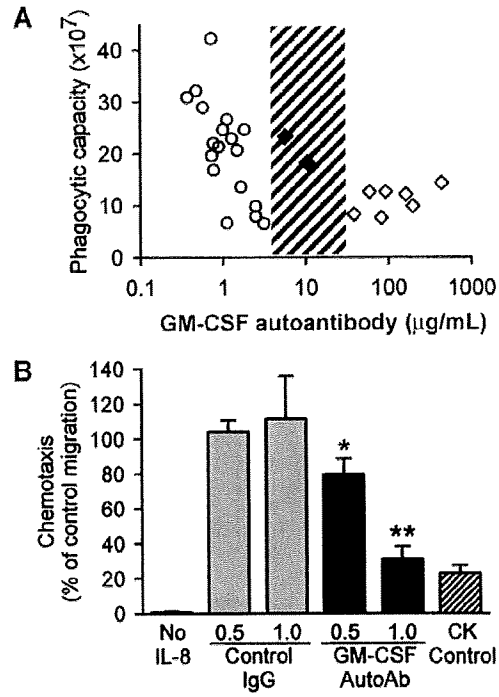

Figure 4. Correlation of GM-CSF autoantibody level and basal neutrophil function in vivo, and effects of GM-CSF autoantibody level on neutrophil function in vitro. (A) The phagocytic capacity of unstimulated neutrophils in whole blood was measured in healthy subjects (○), patients with PAP with active disease (◇), and patients with PAP in clinical remission of the lung disease (♦) by quantifying the uptake of IgG-opsonized latex microspheres as described under "Methods." The range of serum GM-CSF autoantibody levels separating healthy subjects and patients with PAP with active disease evaluated with this assay is indicated (3.2-39 μg /mL, ▨). Each symbol represents the results for triplicate determinations for one subject. The mean (IQR) free serum GM-CSF in healthy subjects was 0.00 (0.00-0.267) pg/mL serum and did not correlate with the neutrophil phagocytic capacity ($P > .05$), whereas GM-CSF autoantibody levels (1.07 [0.74-1.66] μg/mL) correlated with neutrophil phagocytic capacity ($R^2 = -0.70$, $P = .001$) (Spearman rank order correlation). (B) Neutrophil chemotaxis was measured as described in "Methods." In brief, neutrophils were placed in the upper chamber of a transwell culture plate and IL-8 (10 ng/mL) was placed in the lower chamber, both the upper and lower chambers (chemokinesis [CK] control) or was omitted (No IL-8) and GM-CSF autoantibody (0.5, or 1.0 μg/mL) or isotype control antibody (0.5 or 1.0 μg/mL) was placed in the upper chamber. Each bar represents the mean (± SE) for results from 3 determinations. Compared with the respective isotype antibody controls, increasing concentrations of GM-CSF autoantibody reduced neutrophil chemotaxis in rheostatic fashion (*$P < .05$; **$P < .005$).

macrophages by GM-CSF secreted from adjacent respiratory epithelial cells,[4,19,39] the level of GM-CSF autoantibodies associated with development of lung disease is unknown. Therefore, we measured serum GM-CSF autoantibody concentrations in healthy persons and in patients with active PAP lung disease. The critical threshold of serum GM-CSF autoantibodies associated with active PAP lung disease was between 8.5 and 19 μg/mL (Figure 5). It is noteworthy that 2 patients in remission of PAP lung disease at the time of evaluation had serum GM-CSF autoantibody levels of 5.7 and 10.4 μg/mL. Thus, the minimum serum level of GM-CSF autoantibodies associated with the presence of active lung disease in PAP lies between 10.4 and 19 μg/mL.

Discussion

Here, we demonstrate that GM-CSF autoantibodies are normally present in healthy human subjects, albeit at levels lower than in

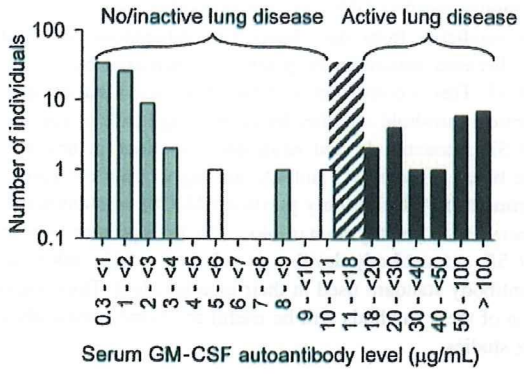

Figure 5. Histogram showing the frequency distribution of serum GM-CSF autoantibody levels in healthy subjects (□, n = 72), patients with PAP with active lung disease (■, n = 21), and patients with PAP in clinical remission of the lung disease (□, n = 2). Clinical remission was defined as formerly diagnosed patients with PAP who were currently presenting no respiratory insufficiency and had normal chest X-ray images. The range of serum GM-CSF autoantibody levels separating subjects with no or active lung disease from those without active disease is indicated (10.4-19 μg/mL, ▨).

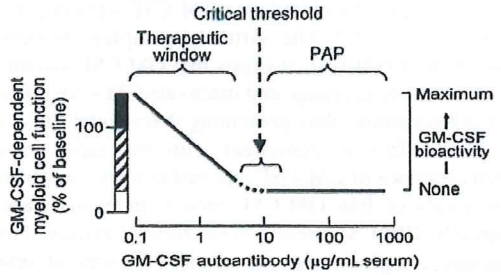

Figure 6. Schematic of the proposed mechanism of innate immune regulation by GM-CSF autoantibodies showing the relationship between endogenous GM-CSF autoantibody level (abscissa), GM-CSF–dependent myeloid cell functions, and GM-CSF bioactivity (ordinate). More than a range of low autoantibody levels present in healthy subjects, myeloid cell functions vary inversely with level of GM-CSF autoantibodies (ordinate, ▨) and increased levels of GM-CSF (eg, present at inflammatory sites or from exogenous administration) increase myeloid cell functions above baseline levels by a mechanism known as "GM-CSF priming" (ordinate, ■). At and above GM-CSF autoantibody levels sufficient to completely neutralize GM-CSF bioactivity (eg, the critical threshold), GM-CSF–stimulated myeloid cell functions are minimal or zero (ordinate, □) and the risk of PAP is increased.

patients with PAP. GM-CSF autoantibody levels correlated inversely with neutrophil functions in vivo and reduced neutrophil functions rheostatically in vitro. GM-CSF was far more abundant in healthy human serum than previously reported[12,13]; however, more than 99% was bound and inactivated by GM-CSF autoantibodies. Although the majority of serum GM-CSF was undetectable with a commercial ELISA kit, it was readily detected with a novel ELISA developed to measure both free and autoantibody-bound GM-CSF. We measured the critical threshold of GM-CSF autoantibodies associated with the presence of PAP. We conclude that GM-CSF autoantibodies scavenge free GM-CSF in vivo and may negatively modulate myeloid cell functions in health and disease.

The observation that GM-CSF autoantibodies are ubiquitous in healthy subjects has implications for the pathogenesis of PAP, suggesting it is caused by a pathologic increase in the level of preexisting GM-CSF autoantibodies rather than a new adaptive antibody response. This is supported by several findings, including that: (1) low levels of GM-CSF autoantibodies were present in all healthy persons evaluated, were inversely correlated with the CD11b stimulation index and basal neutrophil phagocytic function in vivo, and reduced the CD11b stimulation index and neutrophil chemotaxis in vitro; (2) GM-CSF autoantibodies from healthy subjects (from IVIG) and from patients with PAP reduced GM-CSF signaling in vitro to a similar degree; (3) at levels above a critical threshold, GM-CSF autoantibodies were associated with multiple simultaneously impaired GM-CSF–dependent myeloid functions; (4) GM-CSF autoantibodies were specific; (5) other anti-cytokine or noncytokine autoantibodies have not been reported in patients with PAP[20]; and (6) PAP does not occur as a complication of other more common autoimmune diseases.[27,40] Our experimental measurement of the critical threshold of GM-CSF autoantibodies associated with the presence of PAP lung disease showed it lies between 10.4 and 19 μg/mL. This agrees well with our prior estimate of 8-22 μg/mL[26] calculated from data for 1258 healthy subjects,[25] 425 patients with autoimmune diseases but without PAP,[40] and 158 patients with autoimmune PAP.[4] GM-CSF autoantibodies were distinct from the recently identified soluble GM-CSF receptor,[41] which differs in molecular weight and was not detected by far-Western blotting or by liquid chromatography and mass spectroscopy of the GM-CSF-binding band seen in the serum of healthy subjects or patients with PAP. Our study does not rule out that GM-CSF autoantibodies in healthy subjects and patients with PAP may differ in ways important to PAP pathogenesis. Examples of such potential differences include the GM-CSF epitopes targeted, the binding affinity of GM-CSF autoantibodies,[20] or the relative composition of neutralizing and non-neutralizing GM-CSF autoantibodies in healthy subjects and patients with PAP. Future studies focused on these questions and the mechanism of immune dysregulation responsible for increasing the GM-CSF autoantibody level in autoimmune PAP will be important in furthering our understanding of its pathogenesis.

These results predict a novel mechanism of innate immune regulation (Figure 6). In healthy persons, low levels of endogenous GM-CSF autoantibodies determine the ambient level of GM-CSF bioactivity, which determines the basal level of myeloid cell functions. Endogenous myeloid cell priming varies inversely with autoantibody concentration up to the critical threshold. Myeloid cell functions likely regulated by this mechanism include: surfactant catabolism, cell adhesion, phagocytosis, microbial killing, pathogen receptor expression, Toll-like receptor 4 signaling, and others.[1,5] In patients with PAP, very high levels of GM-CSF autoantibodies reduce GM-CSF bioactivity to zero,[20] thereby eliminating GM-CSF priming of myeloid cell functions. This model is consistent with reports that administration of exogenous GM-CSF antibody rheostatically reduces myeloid cell functions in vivo in mice[42] and ex vivo in human blood.[5] It is also consistent with the observation that GM-CSF bioactivity is undetectable in patients with PAP.[20] Because surfactant clearance by alveolar macrophages requires GM-CSF and GM-CSF bioactivity is eliminated at all autoantibody concentrations above the critical threshold, this model explains the lack of correlation between the level of GM-CSF autoantibody and the severity of lung disease in patients with PAP.[31] It also supports the interesting hypothesis of Bendtzen and colleagues (Svenson et al,[25] Ross et al,[43] and Metcalf et al[44]), who first proposed that the therapeutic effects of IVIG may be due to GM-CSF autoantibodies that may function by reducing GM-CSF stimulated myeloid cell reactivity.

Although multiple lines of evidence support the conclusion that GM-CSF autoantibodies are present in healthy subjects, their potential role in immune regulation is less certain. Our current and reported observations strongly support a role for GM-CSF in the constitutive regulation of myeloid cell functions in vivo and suggest that GM-CSF autoantibodies may be

important in negatively modulating GM-CSF signaling in health and disease.[1-4,20,23,24,26] The virtually complete binding and neutralization of GM-CSF suggests that GM-CSF autoantibodies may function to scavenge and inactivate GM-CSF released at sites of inflammation, thus preventing detrimental distal endocrine effects. This is consistent with the rapid, receptor-mediated clearance of GM-CSF reported in mice[45] and also with the low levels of free GM-CSF present in human serum.[5,13] Alternatively, GM-CSF present in the form of inactive circulating immune complexes may be released at sites of infection (perhaps by a drop in pH), where it could stimulate myeloid functions by locking the GM-CSF receptor into its high STAT5-mediated signaling state,[12] thereby amplifying local innate immunity on a microscopic scale. This is consistent with the observation that anti-cytokine antibody binding prolongs the half-life of interleukin-4 in vivo.[46]

Several observations have identified GM-CSF as a molecular target for therapeutic development,[22,23,47-49] including the failure of GM-CSF knockout mice to develop the typical lesions of arthritis or multiple sclerosis in experimental models of these diseases as well as the pathogenic implications of increased local levels of GM-CSF at sites of disease in rheumatoid arthritis. Administration of GM-CSF autoantibody at doses below the critical threshold may rheostatically reduce myeloid cell activity,[5,42] potentially reducing the severity of inflammatory and autoimmune disorders.[24] However, doses exceeding the critical threshold may result in excessive myeloid cell suppression and unwanted clinical manifestations, including alveolar proteinosis and impaired antimicrobial host defenses. Thus, our estimate of the critical threshold helps to define the therapeutic window for the safe use of GM-CSF autoantibodies in potential new clinical therapies. The close agreement of estimates based on various myeloid functions suggests that serum GM-CSF autoantibody levels below 10 μg/mL may not result in adverse clinical manifestations. However, it is also possible that different critical threshold values may exist for distinct GM-CSF–regulated myeloid cell functions (eg, surfactant catabolism, antimicrobial host defense functions), different modes of GM-CSF signaling (eg, endocrine, autocrine, and paracrine), or various tissue compartments (eg, lung versus blood). For example, a lower concentration of GM-CSF is required for maintenance of alveolar macrophage-mediated surfactant clearance than for normal alveolar macrophage immune functions (B.C.C. and B.C.T., unpublished observations). Separately, it is possible that clinically safe levels of very highly purified GM-CSF autoantibodies may be lower than levels predicted from data based on endogenous autoantibody levels because autoantibody potency is increased by removal of GM-CSF. This is consistent with the observation that estimates of the critical threshold obtained by correlating levels of endogenous GM-CSF autoantibody and neutrophil functions in unstimulated whole blood (Figures 3G and 4A) are higher than estimates from experiments in which highly purified GM-CSF autoantibodies are incubated with healthy human blood.[5] It is important to note that GM-CSF autoantibody levels are relative values linked to the autoantibody standard used in their measurement. Thus, standardization of these methods will be useful to ensure comparability of future studies.

Acknowledgments

We thank Jonathan Puchalski, John Howington, and Michael Reed (University of Cincinnati Medical Center, Cincinnati, OH) for help with the care of patients with PAP and clinical sample collection, and Drs. Jeffrey Whitsett, Fred Finkelman, and Christopher Karp (Cincinnati Children's Hospital Medical Center, Cincinnati, OH) for their critical reading of the manuscript.

This work was supported by the National Institutes of Health (Bethesda, MD; HL085453 to B.C.T.), National Center for Research Resources (Bethesda, MD; RR019498 to B.C.T.), and the Japan Society for the Promotion of Science (Tokyo, Japan; B19390403 to Y.Y.).

Authorship

Contribution: K.U., K.N., M.W., and B.C.T. designed research; K.U., T.S., D.E.K., and D.C.B. performed research; M.L. provided vital reagents; C.A.S. served as research coordinator and obtained all the clinical samples from normal volunteers; J.P.K., K.U., and B.C.T. analyzed the data; and K.U., K.N., B.C.C., L.A.D., N.K., Y.Y., and B.C.T. wrote the manuscript.

Conflict-of-interest disclosure: The authors declare no competing financial interests.

Correspondence: Bruce C. Trapnell, MD, Division of Pulmonary Biology, Cincinnati Children's Hospital Medical Center, 3333 Burnet Avenue, Cincinnati, OH 45229-3039; e-mail: bruce.trapnell@cchmc.org

References

1. Shibata Y, Berclaz PY, Chroneos ZC, Yoshida M, Whitsett JA, Trapnell BC. GM-CSF regulates alveolar macrophage differentiation and innate immunity in the lung through PU. 1. Immunity. 2001; 15:557-567.
2. Hamilton JA, Anderson GP. GM-CSF Biology. Growth Factors. 2004;22:225-231.
3. Trapnell BC, Whitsett JA. GM-CSF regulates pulmonary surfactant homeostasis and alveolar macrophage-mediated innate host defense. Annu Rev Physiol. 2002;64:775-802.
4. Trapnell BC, Whitsett JA, Nakata K. Pulmonary Alveolar Proteinosis. N Engl J Med. 2003;349: 2527-2539.
5. Uchida K, Beck DC, Yamamoto T, et al. GM-CSF autoantibodies and neutrophil dysfunction in pulmonary alveolar proteinosis. N Engl J Med. 2007; 356:567-579.
6. Ruef C, Coleman DL. Granulocyte-macrophage colony-stimulating factor: pleiotropic cytokine with potential clinical usefulness. Rev Infect Dis. 1990; 12:41-62.
7. Huffman Reed JA, Rice WR, Zsengeller ZK, Wert SE, Dranoff G, Whitsett JA. GM-CSF enhances lung growth and causes alveolar type II epithelial cell hyperplasia in transgenic mice. Am J Physiol. 1997;273:L715-725.
8. Freedman MH, Grunberger T, Correa P, Axelrad AA, Dube ID, Cohen A. Autocrine and paracrine growth control by granulocyte-monocyte colony-stimulating factor of acute lymphoblastic leukemia cells. Blood. 1993;81:3068-3075.
9. Yamaoka K, Otsuka T, Niiro H, et al. Activation of STAT5 by lipopolysaccharide through granulocyte-macrophage colony-stimulating factor production in human monocytes. J Immunol. 1998; 160:838-845.
10. Graves V, Gabig T, McCarthy L, Strour EF, Leemhuis T, English D. Simultaneous mobilization of Mac-1 (CD11b/CD18) and formyl peptide chemoattractant receptors in human neutrophils. Blood. 1992;80:776-787.
11. Hansen G, Hercus TR, McClure BJ, et al. The structure of the GM-CSF receptor complex reveals a distinct mode of cytokine receptor activation. Cell. 2008;134:496-507.
12. Guthridge MA, Powell JA, Barry EF, et al. Growth factor pleiotropy is controlled by a receptor Tyr/Ser motif that acts as a binary switch. EMBO J. 2006;25:479-489.
13. Carraway MS, Ghio AJ, Carter JD, Piantadosi CA. Detection of granulocyte-macrophage colony-stimulating factor in patients with pulmonary alveolar proteinosis. Am J Respir Crit Care Med. 2000;161:1294-1299.
14. Dranoff G, Crawford AD, Sadelain M, et al. Involvement of granulocyte-macrophage colony-stimulating factor in pulmonary homeostasis. Science. 1994;264:713-716.
15. Stanley E, Lieschke GJ, Grail D, et al. Granulocyte/macrophage colony-stimulating factor-deficient mice show no major perturbation of hematopoiesis but develop a characteristic pulmonary pathology. Proc Natl Acad Sci U S A. 1994;91: 5592-5596.

16. Ikegami M, Ueda T, Hull W, et al. Surfactant metabolism in transgenic mice after granulocyte macrophage-colony stimulating factor ablation. Am J Physiol. 1996;270:L650-658.
17. Seymour JF, Lieschke GJ, Grail D, Quilici C, Hodgson G, Dunn AR. Mice lacking both granulocyte colony-stimulating factor (CSF) and granulocyte-macrophage CSF have impaired reproductive capacity, perturbed neonatal granulopoiesis, lung disease, amyloidosis, and reduced long-term survival. Blood. 1997;90:3037-3049.
18. Seymour JF, Presneill JJ. Pulmonary alveolar proteinosis: progress in the first 44 years. Am J Respir Crit Care Med. 2002;166:215-235.
19. Kitamura T, Tanaka N, Watanabe J, et al. Idiopathic pulmonary alveolar proteinosis as an autoimmune disease with neutralizing antibody against granulocyte/macrophage colony-stimulating factor. J Exp Med. 1999;190:875-880.
20. Uchida K, Nakata K, Trapnell BC, et al. High-affinity autoantibodies specifically eliminate granulocyte-macrophage colony-stimulating factor activity in the lungs of patients with idiopathic pulmonary alveolar proteinosis. Blood. 2004;103:1089-1098.
21. Lang RA, Metcalf D, Cuthbertson RA, et al. Transgenic mice expressing a hemopoietic growth factor gene (GM-CSF) develop accumulations of macrophages, blindness, and a fatal syndrome of tissue damage. Cell. 1987;51:675-686.
22. Jang J, Lim DS, Choi YE, et al. MLN51 and GM-CSF involvement in the proliferation of fibroblast-like synoviocytes in the pathogenesis of rheumatoid arthritis. Arthritis Res Ther. 2006;8:R170.
23. McQualter JL, Darwiche R, Ewing C, et al. Granulocyte macrophage colony-stimulating factor: a new putative therapeutic target in multiple sclerosis. J Exp Med. 2001;194:873-882.
24. Hamilton JA. GM-CSF in inflammation and autoimmunity. Trends Immunol. 2002;23:403-408.
25. Svenson M, Hansen MB, Ross C, et al. Antibody to granulocyte-macrophage colony-stimulating factor is a dominant anti-cytokine activity in human IgG preparations. Blood. 1998;91:2054-2061.
26. Bendtzen K, Svenson M, Hansen MB, et al. GM-CSF autoantibodies in pulmonary alveolar proteinosis. N Engl J Med. 2007;356:2001-2002.
27. Inoue Y, Trapnell BC, Tazawa R, et al. Characteristics of a large cohort of autoimmune pulmonary alveolar proteinosis patients in Japan. Am J Respir Crit Care Med. 2008.
28. Kurdowska A, Miller EJ, Noble JM, et al. Anti-IL-8 autoantibodies in alveolar fluid from patients with the adult respiratory distress syndrome. J Immunol. 1996;157:2699-2706.
29. Watanabe M, Uchida K, Nakagaki K, et al. Anticytokine autoantibodies are ubiquitous in healthy individuals. FEBS Lett. 2007;581:2017-2021.
30. Kitamura T, Uchida K, Tanaka N, et al. Serological diagnosis of idiopathic pulmonary alveolar proteinosis. Am J Respir Crit Care Med. 2000;162:658-662.
31. Seymour JF, Doyle IR, Nakata K, et al. Relationship of anti-GM-CSF antibody concentration, surfactant protein A and B levels, and serum LDH to pulmonary parameters and response to GM-CSF therapy in patients with idiopathic alveolar proteinosis. Thorax. 2003;58:252-257.
32. Berclaz PY, Shibata Y, Whitsett JA, Trapnell BC. GM-CSF, via PU. 1, regulates alveolar macrophage Fcgamma R-mediated phagocytosis and the IL-18/IFN-gamma -mediated molecular connection between innate and adaptive immunity in the lung. Blood. 2002;100:4193-4200.
33. Perkins DN, Pappin DJ, Creasy DM, Cottrell JS. Probability-based protein identification by searching sequence databases using mass spectrometry data. Electrophoresis. 1999;20:3551-3567.
34. Mascot Search: Matrix Science Ltd.; 1997.
35. Steindl F, Armbruster C, Pierer K, Purtscher M, Katinger HW. A simple and robust method for the complete dissociation of HIV-1 p24 and other antigens from immune complexes in serum and plasma samples. J Immunol Methods. 1998;217:143-151.
36. Zsengeller Z, Otake K, Hossain SA, Berclaz PY, Trapnell BC. Internalization of adenovirus by alveolar macrophages initiates early proinflammatory signaling during acute respiratory tract infection. J Virol. 2000;74:9655-9667.
37. Berclaz PY, Zsengeller Z, Shibata Y, et al. Endocytic internalization of adenovirus, nonspecific phagocytosis, and cytoskeletal organization are coordinately regulated in alveolar macrophages by GM-CSF and PU. 1. J Immunol. 2002;169:6332-6342.
38. Gonzalez-Juarrero M, Hattle JM, Izzo A, et al. Disruption of granulocyte macrophage-colony stimulating factor production in the lungs severely affects the ability of mice to control Mycobacterium tuberculosis infection. J Leukoc Biol. 2005;77:914-922.
39. Presneill JJ, Nakata K, Inoue Y, Seymour JF. Pulmonary alveolar proteinosis. Clin Chest Med. 2004;25:593-613, viii.
40. Meager A, Wadhwa M, Bird C, et al. Spontaneously occurring neutralizing antibodies against granulocyte-macrophage colony-stimulating factor in patients with autoimmune disease. Immunology. 1999;97:526-532.
41. Sayani F, Montero-Julian FA, Ranchin V, et al. Identification of the soluble granulocyte-macrophage colony stimulating factor receptor protein in vivo. Blood. 2000;95:461-469.
42. Bozinovski S, Jones J, Beavitt SJ, Cook AD, Hamilton JA, Anderson GP. Innate immune responses to LPS in mouse lung are suppressed and reversed by neutralization of GM-CSF via repression of TLR-4. Am J Physiol Lung Cell Mol Physiol. 2004;286:L877-885.
43. Ross C, Svenson M, Hansen MB, Vejlsgaard GL, Bendtzen K. High avidity IFN-neutralizing antibodies in pharmaceutically prepared human IgG. J Clin Invest. 1995;95:1974-1978.
44. Bendtzen K, Hansen MB, Ross C, Svenson M. High-avidity autoantibodies to cytokines. Immunol Today. 1998;19:209-211.
45. Metcalf D, Nicola NA, Mifsud S, Di Rago L. Receptor clearance obscures the magnitude of granulocyte-macrophage colony-stimulating factor responses in mice to endotoxin or local infections. Blood. 1999;93:1579-1585.
46. Finkelman FD, Madden KB, Morris SC, et al. Anticytokine antibodies as carrier proteins. Prolongation of in vivo effects of exogenous cytokines by injection of cytokine-anti-cytokine antibody complexes. J Immunol. 1993;151:1235-1244.
47. Zaheer A, Zaheer S, Sahu SK, Yang B, Lim R. Reduced severity of experimental autoimmune encephalomyelitis in GMF-deficient mice. Neurochem Res. 2007;32:39-47.
48. Ponomarev ED, Shriver LP, Maresz K, Pedras-Vasconcelos J, Verthelyi D, Dittel BN. GM-CSF production by autoreactive T cells is required for the activation of microglial cells and the onset of experimental autoimmune encephalomyelitis. J Immunol. 2007;178:39-48.
49. Krinner EM, Raum T, Petsch S, et al. A human monoclonal IgG1 potently neutralizing the pro-inflammatory cytokine GM-CSF. Mol Immunol. 2007;44:916-925.

Identification of *MICA* as a Susceptibility Gene for Pulmonary *Mycobacterium avium* Complex Infection

Junko Shojima,[1,a] Goh Tanaka,[1,a] Naoto Keicho,[1] Gen Tamiya,[7] Satoshi Ando,[7] Akira Oka,[8] Yoshikazu Inoue,[9] Katsuhiro Suzuki,[9] Mitsunori Sakatani,[9] Masaji Okada,[9] Nobuyuki Kobayashi,[3] Emiko Toyota,[5] Koichiro Kudo,[3] Akira Kajiki,[10] Hideaki Nagai,[5] Atsuyuki Kurashima,[5] Norihiro Oketani,[11] Hiroshi Hayakawa,[13] Tamiko Takemura,[6] Koh Nakata,[12] Hideyuki Ito,[2] Takatomo Morita,[2] Ikumi Matsushita,[1] Minako Hijikata,[1] Shinsaku Sakurada,[1] Takehiko Sasazuki,[4] and Hidetoshi Inoko[8]

[1]Department of Respiratory Diseases, Research Institute, [2]Department of Thoracic Surgery, and [3]Division of Respiratory Disease, [4]International Medical Center of Japan, [5]National Hospital Organization (NHO) Tokyo Hospital, and [6]Department of Pathology, Japanese Red Cross Medical Center, Tokyo, [7]Department of Clinical Neuroscience, Institute of Health Biosciences, University of Tokushima, Graduate School, Tokushima, [8]Department of Molecular Life Science, Course of Basic Science and Molecular Medicine, Tokai University School of Medicine, Isehara, [9]NHO Kinki-Chuo Chest Medical Center, Sakai, [10]NHO Omuta Hospital, Omuta, [11]NHO Nishi-Niigata Chuo Hospital and [12]Bioscience Medical Research Center, Niigata University, Niigata, and [13]NHO Tenryu Hospital, Hamamatsu, Japan

Host genetic susceptibility to adult pulmonary *Mycobacterium avium* complex disease remains unknown. To identify genetic loci for the disease, we prepared 3 sets of pooled DNA samples from 300 patients and 300 sex-matched control subjects and genotyped 19,651 microsatellite markers in a case-control manner. D6S0009i—located in the *MICA* (major histocompatibility complex class I chain–related A) gene, which encodes a ligand of the NKG2D receptor—had the lowest *P* value in pooled and individual DNA typing. The A6 allele of the microsatellite was significantly associated with female patients ($P < .001$), whereas the classical *HLA-B* and *HLA-DRB1* alleles did not show significant association. Functional analysis of allelic expression imbalance revealed that A6-derived messenger RNA was more highly expressed than non–A6-derived messenger RNA in human bronchial epithelial cells. MICA was expressed in bronchiolar epithelium, alveolar macrophages, and granulomatous lesions. These findings suggest that MICA might be one of the immune molecules affecting the pathogenesis of the disease.

Mycobacterium avium complex (MAC) exists in a natural environment, such as water, soil, and dust [1]. MAC infection causes disseminated disease in immmunocompromised hosts but is also known to cause pulmonary disease in individuals without systemic immunosuppression; patients with chronic lung diseases, such as sequelae of tuberculosis and cystic fibrosis, develop the disease, probably because of impaired local defense mechanisms [2, 3]. Apparently healthy middle-aged to elderly women also contract MAC disease with typical granulomatous inflammation and localized bronchiectasis [4–7]. These lesions often spread and impair pulmonary function. Severe cases are thus fatal, owing to the lack of effective therapeutic measures [4, 8].

Pulmonary MAC disease is not common. The incidence rate is <5 cases per 100,000 according to a report from Japan [2], although detailed epidemiological information is lacking worldwide. Together with possible environmental or bacterial risk factors, these otherwise healthy patients might have genetic susceptibility to the disease. In fact, genetic defects of interferon-γ or interleukin-12 receptors have been reported to be responsible for the disseminated form of the disease in young pediatric patients [9–11], but pathophysiologic analysis in adult sporadic disease has been limited. To date, by analogy with susceptibility to tuberculosis, *HLA* [12–14] and natural resistance–associated macrophage

Received 20 October 2008; accepted 18 December 2008; electronically published 28 April 2009.

Potential conflicts of interest: none reported.

Presented in part: 46th Annual Meeting of the Japanese Respiratory Society, Tokyo, 1–3 June 2006 (abstract OP511).

Financial support: Ministry of Education, Culture, Sports, Science, and Technology of Japan (grants-in-aid for scientific research on priority areas, 2001–2005); National Hospital Organization of Japan (grant for category network).

[a] J.S. and G.T. contributed equally to this work.

Reprints or correspondence: Dr. Naoto Keicho, Dept. of Respiratory Diseases, Research Institute, International Medical Center of Japan, Toyama, Shinjuku-ku, Tokyo, 162-8655, Japan (nkeicho-tky@umin.ac.jp).

The Journal of Infectious Diseases 2009; 199:1707–15

0022-1899/2009/19911-0020$15.00
DOI: 10.1086/598982

protein 1 genes [15] have been investigated, with inconclusive results.

We conducted a multicenter study and collected 300 DNA samples from Japanese patients with pulmonary MAC infection to determine candidate regions in a case-control manner. Unlike recent single-nucleotide polymorphism (SNP)–based genome-wide association studies, which have utilized haplotype tag SNPs [16], the present study started with 3 sequential screenings of pooled DNA samples, which included the typing of 19,651 multiallelic microsatellite markers distributed on the human genome, and ended with individual typing of positive markers. This microsatellite-based approach has already identified candidate susceptibility regions for complex genetic diseases in other studies [17–19], and its advantages and drawbacks have also been discussed in detail elsewhere [17]. We conclude that one of the immune-related genes, *MICA* (major histocompatibility complex class I chain-related A) [20], might be involved in the development of the mycobacterial infectious disease.

METHODS

Case patients. A total of 300 unrelated Japanese patients with pulmonary MAC disease were recruited in 2001–2004 at Kinki-Chuo Chest Medical Center (100 patients), International Medical Center of Japan (97 patients), National Hospital Organization (NHO) Omuta Hospital (58 patients), NHO Tokyo Hospital (25 patients), and NHO Nishi-Niigata Chuo Hospital (20 patients). The average age at onset was 63.4 years, and the male-to-female ratio was ~1:3. Pulmonary MAC infection was diagnosed on the basis of the 1997 American Thoracic Society statement [21]; in brief, all patients had clinical manifestations, small nodules with or without bronchiectasis on computed tomographic images, and bacteriologically definite MAC infection. Patients with or without underlying diseases were enrolled, but those with obviously immunodeficient states (e.g., hematological malignancy, receipt of immunosuppressive therapy, and HIV infection) were excluded. Cultured mycobacterial species were differentiated using a polymerase chain reaction (PCR) kit (Amplicor *Mycobacterium* tests; Roche Diagnostics). Clinical profiles and backgrounds of all subjects were extracted from medical records and interviews conducted by trained medical staff. Samples from all 300 case patients were randomly divided into 3 sets of 100 samples to enable 3-stage screening.

Control subjects. As controls, 2 panels were prepared, consisting of samples from healthy sex-matched Japanese volunteers from the same area. The first panel, which included 300 samples (control group 1), was further divided into 3 sets of 100 samples, to be used for pooled and subsequent individual typing for screening. The second panel, control group 2, which included 494 samples, was obtained mainly from the Health Science Research Resources Bank (Japan Health Sciences Foundation) and used for further individual genotyping of the positive marker. Three hundred sex-matched samples randomly selected from control group 2 were also used for the genotyping of classical *HLA* genes.

Consent/ethics. Written informed consent was obtained from each individual. The present study protocol was approved by the local ethics committees of all participating institutions.

Microsatellite markers, DNA pooling, and typing. We used 19,651 genomewide-designed microsatellite markers, described by Tamiya et al. [17]. Detailed information on microsatellites is available from the Japan Biological Information Research Center (see http://www.jbirc.aist.go.jp/gdbs/). DNA pooling and typing were performed in accordance with the protocol of Tamiya et al. [17]. Each DNA pool contained an equal amount of DNA collected from 100 individual case patients or control subjects. PCR amplification was performed using 96 ng of pooled DNA in a 20-μL reaction solution. The microsatellite typing followed standard protocols using the ABI 3700 DNA analyzer (Applied Biosystems). Peak positions and heights of pooled typing were automatically extracted by the Pick Peak (version 1.7) and Multi Peaks programs developed by Applied Biosystems Japan. After pooled DNA typing of case patients and control subjects was performed 3 times sequentially, positive markers were subsequently investigated by individual genotyping and analyzed by GeneScan (version 3.7) and Genotyper (version 2.0) software (Applied Biosystems).

DNA-based typing of* HLA-B *and HLA-DRB1. DNA-based *HLA* typing was performed using the Luminex Multi-Analyte Profiling System (xMAP technology) with the WAK-Flow HLA Typing Kit (Wakunaga). Polymorphic regions of *HLA* genes were amplified using primer pairs from the kit. Each PCR product was hybridized with allele-specific oligonucleotide probes.

Detection of a large-scale deletion of the* MICA *gene and correction of* MICA *allele frequencies. Large-scale deletion of the human genome is known to cause a null allele of the *MICA* gene, which was exclusively found in HLA-B*4801–carrying individuals in the Japanese population [22]. In microsatellite analysis, heterozygous samples that have this deletion are misidentified as homozygotes of the corresponding allele. Therefore, our individual typing in the D6S0009i marker located in the *MICA* gene had to be corrected by the multiplex PCR method reported elsewhere by Komatsu-Wakui et al. [23] when samples from case patients were compared with samples from control group 2; 2 of the primer pairs are located inside boundaries of the large-scale deletion and produce PCR fragments of 180 and 160 bp, respectively, when the deletion does not exist. On the basis of nucleoside sequences specific to the HLA-B*4801–containing haplotypes, the third primer pair was designed outside the deletion and produces a PCR fragment of 880 bp when the deletion exists.

MICA *gene allelic expression imbalance.* Allele-specific messenger RNA (mRNA) expression by the *MICA* gene was evaluated in bronchial cells isolated from cancer-free bronchi of

the surgically resected lung. Primary cultured bronchial epithelial cells obtained from 42 individuals heterozygous for A6 and non-A6 alleles of D6S0009i marker in the *MICA* gene were tested for allelic expression imbalance, for which a detection method has been well established in principle [24–26]. Briefly, one of the coding SNPs in exon 3 of the *MICA* gene, rs1051790, was used as a marker to distinguish between mRNAs deriving from the A6 allele and those deriving from non-A6 alleles, because the G/C allele of the SNP is in perfect linkage disequilibrium with the A6/non-A6 allele in the Japanese population, according to the IMGT/HLA Sequence Database (http://www.ebi.ac.uk/imgt/hla/align.html) as well as other reports [22, 27].

First, 1 μg of RNA extracted from human bronchial cells was reverse transcribed into complementary DNA (cDNA) using Superscript III reverse transcriptase (Invitrogen) in a 20-μL reaction. For PCR amplification, 2 μL of cDNA was used with AmpliTaq Gold DNA polymerase (Applied Biosystems). Nucleotide sequences of the primer set were 5'-ACCAGGGACTTGACAGGGAACGGAA-3' (forward) and 5'-ATGGGGGGCACTGTTCTCCTCAGGA-3' (reverse). Either of the primers was labeled with fluorescent dye, 6-carboxyfluorescein (Applied Biosystems), to assess the proportion of the corresponding single-stranded fragments. An initial denaturation process at 95°C for 9 min was followed by 35 cycles of 95°C for 15 s, 60°C for 15 s, and 72°C for 30 s and then followed by a final step at 72°C for 7 min. For single-strand conformation polymorphism analysis to separate the 2 alleles, reverse-transcription PCR products were diluted 1:7 in deionized formamide buffer, denatured for 2 min at 94°C, quenched on ice, and loaded onto a glycerol-free 10% polyacrylamide gel. Electorophoresis was done for 3.5 h at 10°C at a constant voltage of 300 V/gel. The relative expression of allele-specific mRNA was quantified on the basis of the difference in band intensities, using the Molecular Imager FX System (Bio-Rad Laboratories) and analysis software (Quantity One 1-D; version 4.5; Bio-Rad Laboratories).

The accuracy of the fluorescence intensity ratio of the PCR products was evaluated in comparison with A6/non-A6 copy numbers of the PCR template: cDNAs of A6 and non-A6 (A9) homozygotes were amplified, respectively, with outer PCR primers MICAoutS (5'-GGGCAGAAGATGTCCTGGGAAATA-3') and MICAoutAS (5'-GACATCCCCCCACTGCTGGGTGTC-3') and cloned into the pCRII-TOPO vector using TOPO TA Cloning Kit Dual Promoter (Invitrogen). A6 and non-A6 plasmid DNAs were isolated by the Qiagen Plasmid Mini Kit (Qiagen), their concentrations were adjusted to 100,000 copies/μL and mixed at various ratios, and then 2 μL of the mixed DNA was subjected to PCR with fluorescence primers, as described above.

Immunohistochemistry. Surgical lung sections were obtained from formalin-fixed paraffin-embedded tissues affected by pulmonary MAC disease ($n = 6$) and from apparently normal tissues completely distinct from cancer lesions ($n = 3$). Surgical sections of colon cancer ($n = 6$) were also prepared as positive controls in which MICA is strongly manifest. After deparaffinization, tissue sections were rehydrated and treated with 1 mmol/L EDTA (pH 8.0) at 95°C for 30 min in an autoclave for antigen retrieval. To detect MICA expression in the tissue, anti-MICA goat polyclonal antibody was applied (2.5 μg/μL; raised against recombinant human MICA extracellular domain; R&D Systems). The equivalent amount of goat immunoglobulin (Ig) G (Immuno-Biological Laboratories) was used as a negative antibody control. After overnight incubation at 4°C, endogenous peroxidase activity was blocked by 0.3% H_2O_2, and the secondary antibody labeled with peroxidase (Histofine Simplestain MAX PO; Nichirei) was added. MICA expression was visualized by use of 3-amino-9-ethyl-carbazole liquid substrate chromogen (Dako), followed by counterstaining with hematoxylin.

Statistical analysis. To calculate *P* values for the screening of pooled samples, we used Fisher's exact test with 2 × 2 contingency tables for each allele and the 2 × *m* contingency table for each locus, where *m* refers to the number of marker alleles observed in a population. Markers for which $P < .05$ were selected as positive at each stage. Allele frequencies in pooled typing were estimated from the heights of peaks. For individual typing, the χ^2 test was used. Haplotypes were estimated by the expectation-maximization method of the Arlequin program (version 3.1; http://lgb.unige.ch/arlequin) and analyzed by the Haploview permutation method (version 3.2; http://www.broad.mit.edu/mpg/haploview/). The 1-sample *t* test was done using JMP statistical discovery software (version 5.0.1; SAS Institute) to assess allelic expression imbalance after logarithmic transformation, comparing observed ratios of allele-specific fluorescence intensity with the expected 1:1 ratio (the null hypothesis).

RESULTS

Genomewide screening for a susceptibility gene for pulmonary MAC disease. Three sets of DNA pools were subjected to genomic screening sequentially. At each stage, microsatellite markers were selected when their *P* values, determined by Fisher's exact test for 2 × 2 or 2 × *m* contingency tables, were <.05. In the first stage, 1296 of 19,651 microsatellites were selected. In the second stage, 263 of the 1296 microsatellites were further extracted. After 3-stage genomewide screening, 42 microsatellites remained. Subsequent individual genotyping further excluded false-positive markers mainly attributable to experimental artifacts in the pooled DNA typing. Eventually, 4 of the 42 microsatellites met the selection criterion; that is, the uncorrected *P* value of a single allele was <.05 in both pooled and individual typing (table 1).

Of the 4 markers, D6S0009i showed the best values ($P < .001$; odds ratio, 1.53 [95% confidence interval, 1.19–1.96]) when all 300 case samples were compared with 300 control samples (con-

Table 1. Allele frequencies of 4 positive microsatellite markers in 300 case patients and 300 control subjects.

Marker	Locus	No. of alleles	No. of positive alleles	Allele frequency, %		P[a]		OR (95% CI)
				Control group 1	Case patients	2 × m	2 × 2	
D11S0536i	11q22.4	3	1	59.2	66.2	.051	.012[b]	1.35 (1.07–1.71)
D13S791	13q22.1	5	3	28.5	21.5	.141	.005[b]	0.69 (0.53–0.89)
D6S0009i/MICA-TM	6p21.3	5	4	26.3	35.3	<.001[b]	<.001[b]	1.53 (1.19–1.96)
D17S1290	17q23.2	8	1	5.2	2.8	.447	.039[b]	0.54 (0.30–0.97)

NOTE. CI , confidence interval; OR, odds ratio.

[a] Fisher's exact test with 2 × 2 or 2 × m contingency tables of alleles (m refers to the no. of marker alleles observed in a population).

[b] $P < .05$.

trol group 1). Indeed, this microsatellite marker was located in the *MICA* gene in the *HLA* region and is known as the MICA-TM polymorphism [28]. Within 100-kb regions upstream and downstream of D11S0536i or D13S791, no genes were identified. D17S1290 was located near the eosinophil peroxidase and lactoperoxidase genes. Because a relationship between gene function and the underlying pathophysiology is not expected at the present time, further analysis of these genes was not considered in the present study.

Allele frequencies of MICA-TM in patients with MAC and another set of control subjects. To address a disease susceptibility gene, we thus selected MICA-TM as a most likely candidate and further compared 300 samples from case patients with another control set of DNA samples (control group 2) by individual typing. We subsequently detected null alleles of *MICA* and discovered 25 null alleles in control subjects and 10 in the case patients. Even after this correction, the A6 allele was more frequent in the case patients ($P = .048$) (table 2). When only female subjects were included, the association was more robust ($P < .001$) (table 3). In the male subgroup, consisting of 74 patients, a significant association was not observed (data not shown).

HLA-B *and* HLA-DRB1 *genotyping.* Association with the *HLA-B* gene was tested because of strong linkage disequilibrium with the *MICA* gene [22, 23]. The *HLA-DRB1* gene was also analyzed because of a reported association with mycobacterial diseases, including MAC disease [12, 13, 29–31]. All 300 case patient and 300 sex-matched control samples randomly chosen from control group 2 were compared. *HLA-B* and *HLA-DRB1* alleles did not show significant association with MAC disease (data not shown). Even when samples from female patients were compared with those from female control subjects, corrected P values did not reach significant levels when multiplied by the number of alleles (table 4), whereas the association with the A6 allele of MICA-TM remained significant (corrected $P = .028$) (data not shown). *HLA* haplotypes were further analyzed, and 2 major haplotypes carrying the A6 allele, B*5201-A6-DRB1*1502 and B*4403-A6-DRB1*1302, were estimated, but these haplotypes were not associated with the disease according to the permutation test (data not shown).

MICA *gene allelic expression imbalance.* To determine whether the amount of *MICA* gene expression differs between A6 and non-A6 alleles, allele-specific mRNA expression of the

Table 2. Allele and genotype frequencies of D6S0009i marker/MICA-TM polymorphisms in 300 case patients and 494 control subjects.

D6S0009i/MICA-TM	Control group 2 (n = 494)		Case patients (n = 300)		P[a]		OR (95% CI)
	No.	Frequency, %	No.	Frequency, %	2 × m	2 × 2	
Alleles					.048[b]		
A4	117	11.8	87	14.5		.125	...
A5	306	31.0	162	27.0		.092	...
A5.1	140	14.2	88	14.7		.784	...
A6	278	28.1	197	32.8		.048[b]	1.25 (1.00–1.55)
A9	122	12.3	56	9.3		.065	...
Null	25	2.5	10	1.7		.319	...
Genotypes					.047[b]		
A6/A6	32	6.4	35	11.7		.011[b]	1.91 (1.16–3.13)
A6/other	214	43.1	127	42.3		.785	...
Other/other	248	50.2	138	46.0		.251	...

NOTE. CI , confidence interval; OR, odds ratio.

[a] χ^2 test with 2 × 2 or 2 × m contingency tables of alleles (m refers to the no. of marker alleles observed in a population).

[b] $P < .05$.

Table 3. Allele and genotype frequencies of D6S0009i marker/MICA-TM polymorphisms in 226 female case patients and 371 female control subjects.

	Female control group 2 (n = 371)		Female case patients (n = 226)		P[a]		
D6S0009i/MICA-TM allele	No.	Frequency, %	No.	Frequency, %	2 × m	2 × 2	OR (95% CI)
Alleles					.005[b]		
A4	91	12.2	58	12.8		.773	...
A5	247	33.2	120	26.5		.014[b]	...
A5.1	98	13.2	66	14.6		.497	...
A6	194	26.2	160	35.4		<.001[b]	1.55 (1.20–1.99)
A9	94	12.7	41	9.1		.057	...
Null	18	2.4	7	1.5		.379	...
Genotypes					.003[b]		
A6/A6	21	5.7	27	11.9		.006[b]	2.26 (1.26–4.05)
A6/other	152	41.0	104	46.0		.227	...
Other/other	198	53.4	95	42.0		.007[b]	...

NOTE. CI , confidence interval; OR, odds ratio.

[a] χ^2 test with 2 × 2 or 2 × m contingency tables of alleles (m refers to the no. of marker alleles observed in a population).

[b] $P < .05$.

MICA gene was evaluated in human cells heterozygous for A6 and non-A6 alleles. This is a method to measure relative amounts of mRNA generated from each of the 2 alleles within each subject, using a genetic marker in the transcribed region of the gene. Allelic expression ratios are considered to represent a more robust phenotypic marker than absolute mRNA levels,

Table 4. Frequencies of *HLA-B* and *HLA-DRB1* alleles in female case patients and control subjects.

	Female controls randomly chosen from control group 2 (n = 225)		Female case patients (n = 226)		
HLA gene	No.	Frequency, %	No.	Frequency, %	P[a]
HLA-B					
B*5201	50	11.1	73	16.2	.026[b]
B*1501	48	10.7	36	8.0	.169
B*5101	42	9.3	49	10.9	.439
B*4002	40	8.9	28	6.2	.130
B*4601	36	8.0	24	5.3	.109
B*3501	34	7.6	21	4.7	.070
B*4403	27	6.0	37	8.2	.195
B*4001	26	5.8	24	5.3	.771
B*5401	26	5.8	32	7.1	.415
B*0702	20	4.4	29	6.4	.186
Other	101	22.4	99	21.9	...
HLA-DRB1					
DRB1*1502	53	11.8	75	16.6	.028[b]
DRB1*0901	53	11.8	68	15.0	.104
DRB1*0405	45	10.0	53	11.7	.254
DRB1*0803	42	9.4	45	10.0	.391
DRB1*1501	38	8.5	27	6.0	.097
DRB1*1302	30	6.7	27	6.0	.358
DRB1*0101	25	5.6	29	6.4	.339
DRB1*0802	25	5.6	17	3.8	.128
Other	139	30.9	111	24.6	...

[a] χ^2 test with 2 × 2 contingency tables of alleles.

[b] $P < .05$.

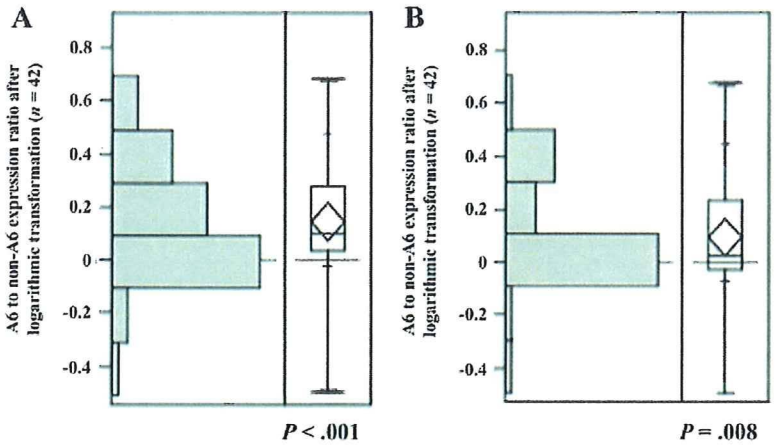

Figure 1. Expression imbalance between A6 and non-A6 alleles. The ratio of A6 to non-A6 expression after logarithmic transformation is shown in the bronchial epithelial cells of 42 heterozygotes. The forward *(A)* and reverse *(B)* primers were labeled with fluorescent dye. The ratio of A6 to non-A6 expression was significantly higher than the expected value of 0, assuming no imbalance after logarithmic transformation by 1-sample *t* test ($P < .001$ for panel A and $P = .008$ for panel B; 1-sample *t* test).

which fluctuate between subjects with changes in cellular environment or *trans*-acting factors [24–26].

First, the validity of the allele-specific ratio in this system was evaluated by measuring the fluorescence intensity of PCR products derived from a mixture of A6 and non-A6 templates at known ratios. The proportion of fluorescence intensity indicating A6-specific expression showed good correlation with the original proportion of A6-derived template when forward or reverse primer was labeled with fluorescent dye ($r^2 = 0.9927$ and $r^2 = 0.9803$, respectively).

Next, the fluorescence intensity of reverse-transcription PCR products from human primary cultured bronchial epithelial cells was measured. The expression ratio of A6 to non-A6 mRNA was 1.6, on average, and the distribution of the ratio after logarithmic transformation was significantly higher than 0, assuming no imbalance between A6-derived and non–A6-derived mRNA expression (figure 1*A*) ($P < .001$). The proportion measured by a fluorescence primer bound to the other strand showed similar results (figure 1*B*) ($P = .008$). These results indicate that the A6 allele is associated with elevated *MICA* mRNA expression levels.

Immunohistochemistry for MICA. Human tissue sections were stained with anti-MICA antibodies. A strong signal was shown in all tested samples from patients with colon cancer, as has been reported by others [32] (figure 2*A* and 2*B*). In the apparently normal lung sections, positive staining was observed in bronchiolar epithelium and alveolar macrophages (figure 2*C* and 2*D*). In addition to the above-described staining, in the lung sections from patients with pulmonary MAC disease, epithelioid cells and multinucleated giant cells composing granuloma were clearly stained with the anti-MICA antibodies (figure 2*E* and 2*F*).

DISCUSSION

We conducted a case-control association study of pulmonary MAC disease, using polymorphic markers distributed genomewide, and we identified *MICA* polymorphism as a susceptible variation. Subsequent gene expression analysis showed localization of *MICA* and possible significance of the allele in the lungs. Thus, *MICA* was found to be one of the promising molecules in pulmonary MAC disease.

With this microsatellite-based approach, Tamiya et al. [17] first showed new susceptible regions for rheumatoid arthritis, and then similar study designs were successfully used to investigate narcolepsy and hypertension [18, 19]. Recently, SNP-based genomewide association analysis achieved very promising results [16, 33], but such a platform was not available when we started the present study. The use of pooled DNA has been discussed as a cost-effective approach with minimal biases and errors when the study is well designed and putative associations are confirmed by individual typing [34].

The reproducibility of our results should be investigated in the future, as in other association studies, because of the following limitations. The *P* values shown by D6S0009i through this analysis are not robust enough when multiple comparisons are taken into account, although Bonferroni's correction might be too conservative to detect associations between multiple marker loci and a complex genetic disease, as has been often discussed elsewhere [35]. We also note that the power to detect risk variants is low with this design, when relative risk is as low as that of the variant (odds ratio, 1.5) identified in this study. Nevertheless, it is noteworthy that MICA is a key molecule in human innate immunity, and the best positive marker within the gene was

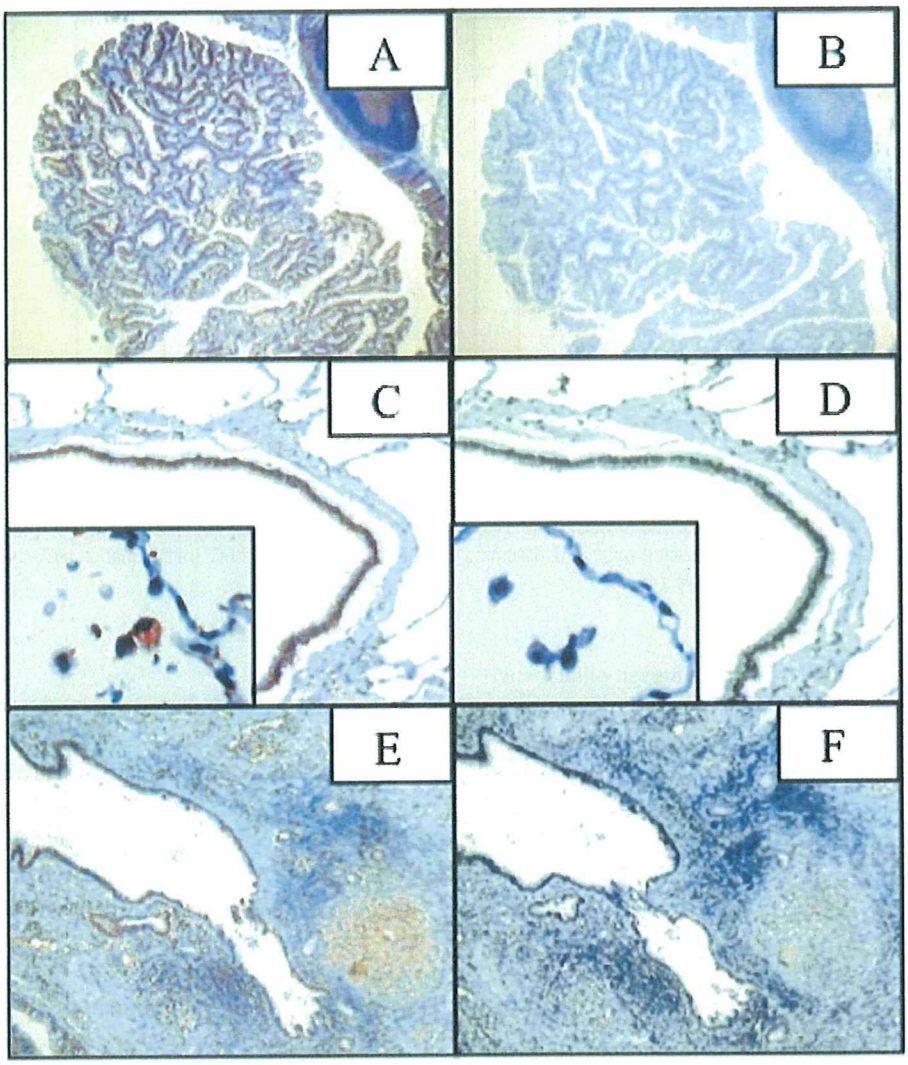

Figure 2. Immunohistochemical staining of MICA (major histocompatibility complex class I chain–related A) in human tissue. The primary antibodies were anti-MICA (extracellular domain) antibody (*A, C,* and *E*) and normal goat immunoglobulin (Ig) G as a negative control (*B, D,* and *F*). *A* and *B,* Colon cancer. *C* and *D,* Lung tissue free of lung cancer. *E* and *F,* Lung lesions of pulmonary *Mycobacterium avium* complex (MAC) disease. MICA was expressed in colon cancer cells *(A).* In apparently normal lung tissue, MICA expression was limited in the bronchiolar epithelium and alveolar macrophages *(C).* In lung tissue from patients with pulmonary MAC disease, epithelioid cells and multinucleated giant cells composing granulomas were clearly stained with anti-MICA antibody, in addition to the staining described for normal tissue *(E).* No staining was seen with goat IgG for the same samples (*B, D,* and *F*). Images are representative images of all tested sections.

identified in a larger sample than in other studies of pulmonary MAC disease [12–15].

In addition, female patients showed a stronger association than did patients of both sexes combined and might be more affected by the combination of host genetic factors, including the *MICA* gene, and putative sex-specific factors, such as hormonal change, which is presumably involved in the female predominance of this disease [4–7, 36]. The number of male patients was rather small and did not provide enough power to detect similar risk in this subgroup.

As reported elsewhere, *HLA-B* and *MICA* are in strong linkage disequilibrium, and *MICA-A6* composes haplotypes with HLA-B*5201, 4403, and 5101. *HLA-DRB1* loci, especially DR2 (DRB1*15) and DR6 (DRB1*13 or *14), have been shown elsewhere to be associated with MAC and other mycobacterial diseases in studies with relatively small samples [12, 14, 29–31]. In our present study, however, disease association with *HLA-B* and *HLA-DRB1* alleles did not reach significant levels, whereas A6 showed a significant association with the disease in the same sample set. Linkage disequilibrium around major A6-containing haplotypes, such as B*5201-A6-DRB1*1502, may explain simply why other studies have shown disease association with classical *HLA* genes [29–31]. Thus, *MICA* should also be considered when *HLA* alleles are associated with mycobacterial diseases.

MICA is functionally known as one of the ligands to engage the NKG2D receptor on natural killer cells, γ-δ T cells, and CD8 T cells. This molecule is a stress-induced, membrane-bound glycoprotein that is expressed in intestinal epithelium and other tissues [37–39]. A recent report showed that MICA is also expressed in human bronchial epithelium [40]. In association studies, frequencies of the A6 allele and HLA-B51 in Behçet's disease [41, 42] and A6 and HLA-B52 in ulcerative colitis [43] are significantly higher than in control populations. In our study, as in others, the A6 allele showed positive association with the disease. The null allele or A5.1 allele, which may impair MICA function, was not associated with the disease, presumably because of functional compensation by other human NKG2D ligands [44].

Our experiment with allelic expression imbalance demonstrated that the constitutive expression of the *MICA* gene in bronchial epithelial cells is genetically determined, at least in part, and that the A6 allele acts as a marker of high MICA expression, although the primary significance of alanine repeats in the transmembraneous region of MICA-TM polymorphism remains unclear. Possible roles of other unknown polymorphisms in linkage disequilibrium with the A6 allele should also be investigated in the future.

MICA was detected by immunohistochemical analysis in alveolar macrophages, epithelioid cells, and multinucleated giant cells in granulomatous lesions of MAC disease as well as in bronchiolar epithelium. This is not surprising, because recent reports have shown that *MICA* is expressed in the monocyte-macrophage lineage as well as in epithelial cells [45–47]. Local macrophages are known to play a critical role in immunity to intracellular pathogens, such as mycobacterial species [48]. These findings imply that the A6 allele or A6 haplotypes might generally provoke inflammatory response or tissue damage, which might be the case with pulmonary mycobacterial diseases, at least in part, although the effect of MICA itself might be relatively weak. Future genetic analysis of other functionally equivalent NKG2D ligands, such as members of the UL-16 binding protein family, might provide an answer concerning this hypothesis [44]. In conclusion, using a genomewide case-control approach and subsequent functional analysis of gene expression, we found that MICA is one of the promising candidate molecules that might be involved in susceptibility to pulmonary MAC disease.

Acknowledgments

We thank Dr. Jun Ohashi and Dr. Naoki Ishizuka for their valuable advice on statistical analysis, Ms. Mei Naganuma and Ms. Tokie Totsu for their excellent technical assistance, and Dr. Kazuko Tanabe for her critical reading of the manuscript.

References

1. Wendt SL, George KL, Parker BC, Gruft H, Falkinham JO III. Epidemiology of infection by nontuberculous mycobacteria. III. Isolation of potentially pathogenic mycobacteria from aerosols. Am Rev Respir Dis **1980**; 122:259–63.
2. Sakatani M. Nontuberculous mycobacteriosis. Kekkaku **1999**; 74:377–84.
3. Henry MT, Inamdar L, O'Riordain D, Schweiger M, Watson JP. Nontuberculous mycobacteria in non-HIV patients: epidemiology, treatment and response. Eur Respir J **2004**; 23:741–6.
4. Prince DS, Peterson DD, Steiner RM, et al. Infection with *Mycobacterium avium* complex in patients without predisposing conditions. N Engl J Med **1989**; 321:863–8.
5. Kennedy TP, Weber DJ. Nontuberculous mycobacteria: an underappreciated cause of geriatric lung disease. Am J Respir Crit Care Med **1994**; 149:1654–8.
6. Reich JM, Johnson RE. *Mycobacterium avium* complex pulmonary disease presenting as an isolated lingular or middle lobe pattern: the Lady Windermere syndrome. Chest **1992**; 101:1605–9.
7. Tanaka E, Kimoto T, Tsuyuguchi K, et al. Effect of clarithromycin regimen for *Mycobacterium avium* complex pulmonary disease. Am J Respir Crit Care Med **1999**; 160:866–72.
8. Field SK, Fisher D, Cowie RL. *Mycobacterium avium* complex pulmonary disease in patients without HIV infection. Chest **2004**; 126:566–81.
9. Newport MJ, Huxley CM, Huston S, et al. A mutation in the interferon-gamma-receptor gene and susceptibility to mycobacterial infection. N Engl J Med **1996**; 335:1941–9.
10. Altare F, Durandy A, Lammas D, et al. Impairment of mycobacterial immunity in human interleukin-12 receptor deficiency. Science **1998**; 280:1432–5.
11. Ottenhoff TH, Verreck FA, Lichtenauer-Kaligis EG, et al. Genetics, cytokines and human infectious disease: lessons from weakly pathogenic mycobacteria and salmonellae. Nat Genet **2002**; 32:97–105.
12. Takahashi M, Ishizaka A, Nakamura H, et al. Specific HLA in pulmonary MAC infection in a Japanese population. Am J Respir Crit Care Med **2000**; 162:316–8.
13. Kubo K, Yamazaki Y, Hanaoka M, et al. Analysis of HLA antigens in *Mycobacterium avium-intracellulare* pulmonary infection. Am J Respir Crit Care Med **2000**; 161:1368–71.
14. Chakraborty AK, Damle PB, Davidson PT, McCalmon RT. Disease due to *Mycobacterium intracellulare*: its possible association with human leukocyte antigens. Rev Infect Dis **1981**; 3:1060–3.
15. Tanaka G, Shojima J, Matsushita I, et al. Pulmonary *Mycobacterium avium* complex infection: association with NRAMP1 polymorphisms. Eur Respir J **2007**; 30:90–6.
16. Wadman, M. Genome miners rush to stake claims. Nature **2007**; 447: 623.
17. Tamiya G, Shinya M, Imanishi T, et al. Whole genome association study of rheumatoid arthritis using 27039 microsatellites. Hum Mol Genet **2005**; 14:2305–21.
18. Kawashima M, Tamiya G, Oka A, et al. Genomewide association analysis of human narcolepsy and a new resistance gene. Am J Hum Genet **2006**; 79:252–63.
19. Yatsu K, Mizuki N, Hirawa N, et al. High-resolution mapping for essential hypertension using microsatellite markers. Hypertension **2007**; 49: 446–52.
20. Bahram S, Bresnahan M, Geraghty DE, Spies T. A second lineage of mammalian major histocompatibility complex class I genes. Proc Natl Acad Sci USA **1994**; 91:6259–63.
21. American Thoracic Society. Diagnosis and treatment of disease caused by nontuberculous mycobacteria. Am J Respir Crit Care Med **1997**; 156: S1–25.
22. Komatsu-Wakui M, Tokunaga K, Ishikawa Y, et al. MIC-A polymorphism in Japanese and a MIC-A-MIC-B null haplotype. Immunogenetics **1999**; 49:620–8.
23. Komatsu-Wakui M, Tokunaga K, Ishikawa Y, et al. Wide distribution of the MICA-MICB null haplotype in East Asians. Tissue Antigens **2001**; 57:1–8.

24. Hirota T, Ieiri I, Takane H, et al. Allelic expression imbalance of the human CYP3A4 gene and individual phenotypic status. Hum Mol Genet **2004**; 13:2959–69.
25. Heighway J, Bowers NL, Smith S, Betticher DC, Koref MF. The use of allelic expression differences to ascertain functional polymorphisms acting in cis: analysis of MMP1 transcripts in normal lung tissue. Ann Hum Genet **2005**; 69:127–3.
26. Caffrey TM, Joachim C, Paracchini S, Esiri MM, Wade-Martins R. Haplotype-specific expression of exon 10 at the human MAPT locus. Hum Mol Genet **2006**; 15:3529–37.
27. Obuchi N, Takahashi M, Nouchi T, et al. Identification of MICA alleles with a long Leu-repeat in the transmembrane region and no cytoplasmic tail due to a frameshift-deletion in exon 4. Tissue Antigens **2001**; 57: 520–35.
28. Mizuki N, Ota M, Kimura M, et al. Triplet repeat polymorphism in the transmembrane region of the MICA gene: a strong association of six GCT repetitions with Behcet disease. Proc Natl Acad Sci USA **1997**; 94: 1298–303.
29. LeBlanc SB, Naik EG, Jacobson L, Kaslow RA. Association of DRB1*1501 with disseminated *Mycobacterium avium* complex infection in North American AIDS patients. Tissue Antigens **2000**; 55:17–23.
30. Fitness J, Tosh K, Hill AV. Genetics of susceptibility to leprosy. Genes Immun **2002**; 3:441–53.
31. Singh SP, Mehra NK, Dingley HB, Pande JN, Vaidya MC. Human leukocyte antigen (HLA)-linked control of susceptibility to pulmonary tuberculosis and association with HLA-DR types. J Infect Dis **1983**; 148: 676–81.
32. Groh V, Rhinehart R, Secrist H, Bauer S, Grabstein KH, Spies T. Broad tumor-associated expression and recognition by tumor-derived gamma delta T cells of MICA and MICB. Proc Natl Acad Sci USA **1999**; 96: 6879–84.
33. Chanock SJ, Manolio T, Boehnke M, Boerwinkle E, Hunter DJ, et al. Replicating genotype-phenotype associations. NCI-NHGRI Working Group on Replication in Association Studies. Nature **2007**; 447:655–60.
34. Sham P, Bader JS, Craig I O'Donovan M, Owen M. DNA Pooling: a tool for large-scale association studies. Nat Rev Genet **2002**; 3:862–71.
35. Devlin B, Roeder K, Wasserman L. Analysis of multilocus models of association. Genet Epidemiol **2003**; 25:36–47.
36. Tsuyuguchi K, Suzuki K, Matsumoto H, Tanaka E, Amitani R, Kuze F. Effect of oestrogen on *Mycobacterium avium* complex pulmonary infection in mice. Clin Exp Immunol **2001**; 123:428–34.
37. Groh V, Steinle A, Bauer S, Spies T. Recognition of stress-induced MHC molecules by intestinal epithelial gammadelta T cells. Science **1998**; 279: 1737–40.
38. Bauer S, Groh V, Wu J, et al. Activation of NK cells and T cells by NKG2D, a receptor for stress-inducible MICA. Science **1999**; 285:727–9.
39. Deng L, Mariuzza RA. Structural basis for recognition of MHC and MHC-like ligands by natural killer cell receptors. Semin Immunol **2006**; 18:159–66.
40. Borchers MT, Harris NL, Wesselkamper SC, Vitucci M, Cosman D. NKG2D ligands are expressed on stressed human airway epithelial cells. Am J Physiol Lung Cell Mol Physiol **2006**; 291:L222–31.
41. Nishiyama M, Takahashi M, Manaka K, Suzuki S, Saito M, Nakae K. Microsatellite polymorphisms of the MICA gene among Japanese patients with Behcet's disease. Can J Ophthalmol **2006**; 41:210–5.
42. Park SH, Park KS, Seo YI, et al. Association of MICA polymorphism with HLA-B51 and disease severity in Korean patients with Behcet's disease. J Korean Med Sci **2002**; 17:366–70.
43. Seki SS, Sugimura K, Ota M, et al. Stratification analysis of MICA triplet repeat polymorphisms and HLA antigens associated with ulcerative colitis in Japanese. Tissue Antigens **2001**; 58:71–6.
44. Raulet DH. Roles of the NKG2D immunoreceptor and its ligands. Nat Rev Immunol **2003**; 3:781–90.
45. Zwirner NW, Fernandez-Vina MA, Stastny P. MICA, a new polymorphic HLA-related antigen, is expressed mainly by keratinocytes, endothelial cells, and monocytes. Immunogenetics **1998**; 47:139–48.
46. Nedvetzki S, Sowinski S, Eagle RA, et al. Reciprocal regulation of human natural killer cells and macrophages associated with distinct immune synapses. Blood **2007**; 109:3776–85.
47. Das H, Groh V, Kuijl C, et al. MICA engagement by human Vgamma2Vdelta2 T cells enhances their antigen-dependent effector function. Immunity **2001**; 15:83–93.
48. Fenton MJ, Vermeulen MW. Immunopathology of tuberculosis: roles of macrophages and monocytes. Infect Immun **1996**; 64:683–90.

OPEN ACCESS Freely available online PLoS one

Prevalence and Risk Factors for Tuberculosis Infection among Hospital Workers in Hanoi, Viet Nam

Luu Thi Lien[1☯], Nguyen Thi Le Hang[2☯], Nobuyuki Kobayashi[3], Hideki Yanai[4], Emiko Toyota[5], Shinsaku Sakurada[6], Pham Huu Thuong[1], Vu Cao Cuong[7], Akiko Nanri[8], Tetsuya Mizoue[8], Ikumi Matsushita[6], Nobuyuki Harada[9], Kazue Higuchi[9], Le Anh Tuan[10], Naoto Keicho[6]*

1 Hanoi Tuberculosis and Lung Disease Hospital, Hanoi, Viet Nam, **2** International Medical Center of Japan - Bach Mai Hospital (IMCJ-BMH) Medical Collaboration Center, Hanoi, Viet Nam, **3** Department of Respiratory Medicine, Toyama Hospital, International Medical Center of Japan, Tokyo, Japan, **4** Institute of Tropical Medicine, Nagasaki University, Nagasaki, Japan, **5** Department of Respiratory Diseases, NHO Tokyo Hospital, Tokyo, Japan, **6** Department of Respiratory Diseases, Research Institute, International Medical Center of Japan, Tokyo, Japan, **7** General Planning Department, Hanoi Tuberculosis and Lung Disease Hospital, Hanoi, Viet Nam, **8** Department of Epidemiology and International Health, Research Institute, International Medical Center of Japan, Tokyo, Japan, **9** Department of Mycobacterium Reference and Research, Research Institute of Tuberculosis, Tokyo, Japan, **10** Hanoi Department of Health, Hanoi, Viet Nam

Abstract

Background: Transmission of tuberculosis (TB) to health care workers (HCWs) is a global issue. Although effective infection control measures are expected to reduce nosocomial TB, HCWs' infection has not been assessed enough in TB high burden countries. We conducted a cross-sectional study to determine the prevalence of TB infection and its risk factors among HCWs in Hanoi, Viet Nam.

Methodology/Principal Findings: A total of 300 HCWs including all staff members in a municipal TB referral hospital received an interferon-gamma release assay (IGRA), QuantiFERON-TB Gold In-Tube™, followed by one- and two-step tuberculin skin test (TST) and a questionnaire-based interview. Agreement between the tests was evaluated by kappa statistics. Risk factors for TB infection were analyzed using a logistic regression model. Among the participants aged from 20 to 58 years (median = 40), prevalence of TB infection estimated by IGRA, one- and two-step TST was 47.3%, 61.1% and 66.3% respectively. Although the levels of overall agreement between IGRA and TST were moderate, the degree of agreement was low in the group with BCG history (kappa = 0.29). Working in TB hospital was associated with twofold increase in odds of TB infection estimated by IGRA. Increased age, low educational level and the high body mass index also demonstrated high odds ratios of IGRA positivity.

Conclusions/Significance: Prevalence of TB infection estimated by either IGRA or TST is high among HCWs in the hospital environment for TB care in Viet Nam and an infection control program should be reinforced. In communities with heterogeneous history of BCG vaccination, IGRA seems to estimate TB infection more accurately than any other criteria using TST.

Citation: Lien LT, Hang NTL, Kobayashi N, Yanai H, Toyota E, et al. (2009) Prevalence and Risk Factors for Tuberculosis Infection among Hospital Workers in Hanoi, Viet Nam. PLoS ONE 4(8): e6798. doi:10.1371/journal.pone.0006798

Editor: Madhukar Pai, McGill University, Canada

Received April 24, 2009; **Accepted** July 27, 2009; **Published** August 27, 2009

Funding: This work was supported by grants from the Program of Founding Research Centers for Emerging and Reemerging Infectious Diseases, MEXT, Japan. The funders had no role in study design, data collection and analysis, decision to publish, or preparation of the manuscript.

Competing Interests: The authors have declared that no competing interests exist.

* E-mail: keicho@ri.imcj.go.jp

☯ These authors contributed equally to this work.

Introduction

Transmission of *Mycobacterium tuberculosis* (MTB) in health care facilities is a problem worldwide [1–3]. Occupational tuberculosis (TB) can lead to the loss of skilled workers and impact health care service adversely, which has serious consequences in association with recent spread of multi-drug resistant (MDR) MTB strains [1]. Effective infection control measures are expected to reduce nosocomial TB [3–6]. In this sense, estimation of prevalence and risk for TB infection among health care workers (HCWs) involved in TB care is one of the essential steps to review and reinforce TB control measures.

In TB high burden countries, however, occupational risk for TB has often been neglected and concealed by the high prevalence in the general population. Furthermore, in those countries, widespread use of BCG vaccination has interfered with interpretation of tuberculin skin testing (TST) [1,7], which was the only measure to detect TB infection until recently.

A newly developed diagnostic test designated as the interferon-gamma release assay (IGRA) uses a principle that MTB-specific antigens provoke immune reaction in the whole blood after TB infection [8]. With the advent of IGRA, many investigators have reported that latent TB infection could be detected more specifically than using TST [9–11]. QuantiFERON-TB Gold test, an ELISA-based IGRA, is also recommended by the US Centers for Disease Control and Prevention (CDC) for initial and sequential-testing of latent TB infection among HCWs [12].

Viet Nam is one of the 22 TB high burden countries defined by WHO, with prevalence of TB being 227/100,000 population and drug resistance TB is ever-increasing [13]. In Hanoi, the capital of Viet Nam, prevalence of smear positive pulmonary TB is 146/100,000 population [14] and the annual risk of TB infection reported from the suburban area is 0.8% [15]. Despite the high burden, little is known about TB infection among HCWs. We conducted this study to estimate the prevalence and risk factors for TB infection among HCWs in a crowded TB referral hospital together with an adjacent general hospital in Hanoi, Viet Nam, by comparing IGRA with conventional TST one- and two-step methods.

Methods

Ethics statement

A written informed consent was obtained from each participant. The study was approved by ethical committees of the Ministry of Health, Viet Nam and International Medical Center of Japan respectively.

Study design and setting

We conducted a cross-sectional study in November 2007 in two hospitals adjacently located in the same block of Hai Ba Trung District in Hanoi city (Figure 1). A 110-bed "TB hospital", which receives 2,000 TB in-patients and 46,000 turns of examination per year, is mainly assigned for taking care of TB patients in the entire city. The other is a 460-bed "non-TB hospital", which is a general hospital but transfers all TB-suspected patients to the aforementioned TB hospital.

Participants and data collection

Sample size was determined by the number of all staff members in the TB hospital, since our goal was to clarify the situation of all available HCWs working in the environment. The same categories of departments, such as outpatient clinic, intensive care unit, departments of internal medicine, laboratory and administration were selected from the non-TB hospital and the equivalent number was randomly extracted from each category. Demographic information, history of BCG vaccination and factors potentially associated with TB exposure were collected by an interview using a structured questionnaire. Those factors included job category, duration of working, practice of wearing mask, and professional or household contact with TB patients. For all participants, the blood was collected for IGRA, then TST was administered but not for those with pregnancy, breast-feeding or allergy to tuberculin. To rule out active TB, chest X-ray was taken for all participants with positive IGRA results. Sputum test was performed for participants with productive cough. They also had the chance of receiving INH for treatment of latent TB infection if they wished, after consultation with TB doctors there.

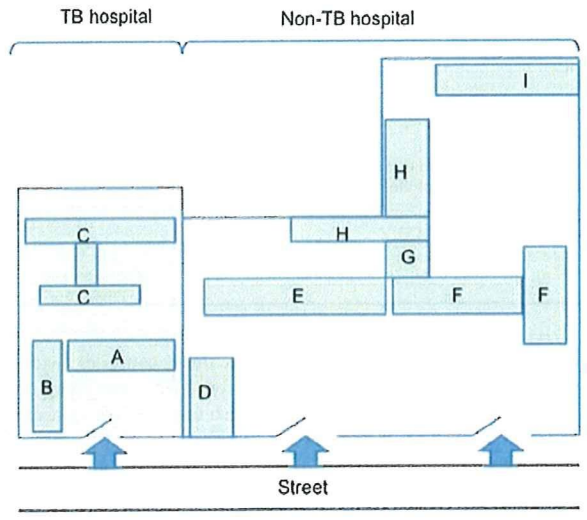

Figure 1. Allocation of two hospitals. TB: Tuberculosis. TB hospital buildings: A=Administration; B=Outpatient clinic and Laboratory; C=Wards and Imaging diagnosis. Non-TB hospital buildings: D=Emergency; E=Wards; F=Laboratory; G=Administration and Imaging diagnosis; H=Out-patient clinic and Wards; I=Imaging diagnosis.
doi:10.1371/journal.pone.0006798.g001

TST and IGRA

As the first TST, a 5-tuberculin unit dose of Purified Protein Derivatives (Pasteur institute, Nha Trang, Viet Nam), authorized by the Ministry of Health of Viet Nam, was administered by well-trained technicians. Diameter of the induration size was measured after 48 to 72 hours, using a standardized ruler. If the size was less than 10 mm, the second administration with the same dosage was given after 14 days and the results were interpreted similarly (the second TST). From experience in Viet Nam [15], a cut-off value of 10 mm was used in this study, unless otherwise specified. Possible effects of changing cut-off values from 11 mm to 15 mm were also evaluated.

IGRA for TB is a method to measure interferon-gamma induced by MTB-specific antigens (TB antigen) to detect infection. In this study, the newest version of ELISA-based IGRA, QuantiFERON-TB Gold In-Tube™ (Cellestis, Victoria, Australia), was used. One milliliter of the whole blood was collected separately in each heparin-containing tube pre-coated with nil for negative control, mitogen for positive control, and TB antigen. After 18-hour incubation in 37°C, each tube was centrifuged and plasma was harvested. Concentration of interferon-gamma in the plasma was measured using the ELISA method and calculated using analytical software recommended by the manufacturer. The cut-off value of interferon-gamma concentration was 0.35 IU/ml calculated from TB antigen minus negative control. Based on the algorithm of the software, the result was considered to be indeterminate in one of the following two conditions: the nil value itself was higher than 8.0 IU/ml, or mitogen minus nil value was less than 0.5 IU/ml in addition to TB antigen minus nil was less than 0.35 IU/ml. The testing procedure was carefully monitored [16] and quality control of the test was done in each run, following the manufacturer's instruction.

Statistical analysis

To compare proportions in two groups, chi-squared test was used. Mantel-Haenszel method for stratified data was also attempted. Agreement between TST and IGRA was quantified using kappa statistic. Symmetry test equivalent to McNemar test was used to evaluate the symmetry of discordant results, TST+/IGRA- and TST-/IGRA+. To determine whether history of BCG vaccination or other factors interprets discordant results, unadjusted and adjusted odds ratios were calculated using a logistic regression model. The associations between potential risk factors and TB infection estimated by IGRA positivity were also evaluated by multivariate analysis using a logistic regression model, with IGRA result as outcome and factors possibly related to tuberculosis infection as independent variables. Biologically significant variables such as sex and other variables showing p

values <0.20 in the univariate analysis were included in the multivariate model. All statistical analyses were performed using Stata version 10 (StataCorp, College Station, TX) and $p<0.05$ was considered to be statistically significant.

Results

Characteristics of study population

As shown in Table S1, a total of 300 HCWs of the two hospitals participated in our study and the majority of these were female. The median age was 40 years old, ranging from 20 to 58. Educational levels depended on job categories, but two thirds were at pre-university level or lower. More than one third of the participants had a history of BCG vaccination, of which more than 95% had actual BCG scar (data not shown).

Participants to the study included all of the 150 HCWs working in the TB hospital and 150 of 803 HCWs from the non-TB hospital (Table S1). Two thirds of HCWs in the TB hospital were less than 40 years old and this proportion was larger than in the non-TB hospital ($p<0.0001$, table not shown).

Study flow

As shown in Figure 2, all 300 participants provided blood for IGRA, while 288 of the 300 received TST. Out of them, 112 (38.9%) HCWs whose induration size of the first TST was less than 10 mm took the second TST. IGRA results were indeterminate in 35 (11.7%) individuals, in which 33 received TST and 2 did not. Since IGRA-TST data sets were analyzable when positive or negative results were obtained from both tests, these 33 IGRA indeterminate results were subtracted from 288 TST results, making 255 valid data sets. For check-up of active pulmonary TB, 131 of 142 IGRA-positive HCWs took chest radiography. Spontaneously cured tuberculosis was not completely excluded in 11 individuals (data not shown). Although active TB could not be ruled out from the chest radiography in one individual, all of the IGRA-positive individuals did not report any signs or symptoms in the follow-up period and were regarded as having latent TB infection. TST results were not emphasized in making this decision, because we expected that false-positive TST results due to previous BCG vaccination were not clinically negligible. None of them agreed to take INH treatment.

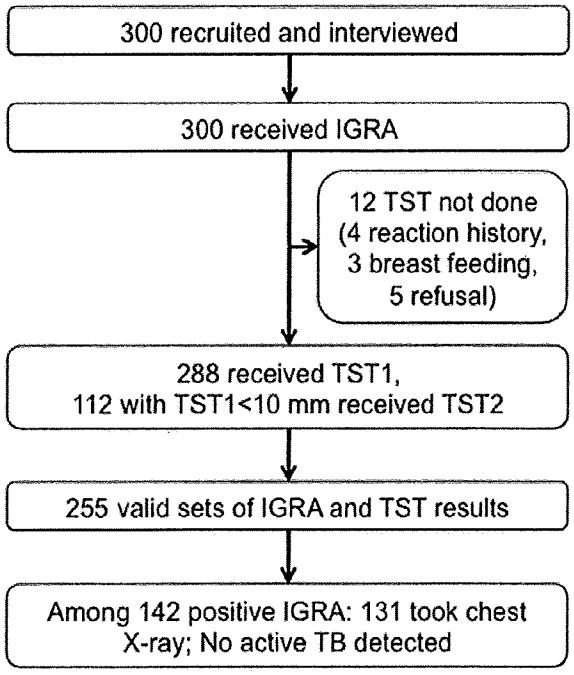

Figure 2. Study flow diagram. IGRA: Interferon-gamma release assay; TST1: The first Tuberculin skin test; TST2: The second Tuberculin skin test; TB: Tuberculosis.
doi:10.1371/journal.pone.0006798.g002

TST and IGRA positivity

TST measurements were obtained in 288 individuals. With a cut-off value of 10 mm, 176 of 288 (61.1%) were positive after the initial injection as a result of conventional "one-step" TST (Table not shown). Of 112 participants with negative TST initially, 15 turned into positive after the second injection, increasing the overall positivity up to 66.3% as a result of "two-step" TST. When 15 mm of induration size was used as the cut-off value, positive results were decreased to half (29.5%). Positive or negative IGRA results were obtained in 265 out of 300 individuals (88.3%). With the cut-off point of IGRA described in the method section, 142 were positive out of the total 300 tested (47.3%).

Since age distribution was rather different between the two hospitals, data stratified by age of each hospital was shown in Table 1. In the TB hospital, positive TST results with one-step TST and 10-mm cut-off value accounted for 54.9%, 72.7%, 86.5% and 85.7% in groups of 20–29, 30–39, 40–49 and ≥50 years old respectively. IGRA results in the same hospital revealed positive in 38.2%, 47.9%, 51.3% and 87.5% for the corresponding age groups. The proportion of TST ≥10 mm was higher in the TB hospital than in the non-TB hospital by the Mantel-Haenszel test. IGRA positivity in the TB hospital had a similar tendency as compared with that in the non-TB hospital when stratified by age, although the difference did not reach statistical significance (Table 1).

Agreement between TST and IGRA

TST using different cut-off values were compared with IGRA in 255 sets of data (Table 2). Overall kappa values showed moderate agreement (kappa = 0.4 to 0.6) between TST and IGRA, whereas high cut-off values such as 13 mm and 15 mm of TST did not further increase the degree of agreement. As compared with one-step TST with the cut-off value of 10 mm (agreement rate = 72.5%, kappa = 0.44), two-step TST did not have any favorable effect on the degree of agreement (agreement rate = 71.0%, kappa = 0.41). In the group with BCG history, the degree of agreement was rather low, in contrast to the group without BCG history (kappa = 0.29 vs. 0.55) (Table 2).

These findings prompted us to investigate the source of disagreement. With the cut-off value of 10 mm, the number of TST+/IGRA- individuals was disproportionately larger than that of TST-/IGRA+ individuals, which was statistically significant by the symmetry test ($p = 0.0008$). This disproportion was predominant in the subgroup with BCG history, but not in that without BCG history ($p = 0.0013$ vs. 0.20 respectively), when the same cut-off value was applied. Conversely, TST-/IGRA+, the other type of discordance, was strikingly increased when cut-off values of 13 or 15-mm were used ($p = 0.0008$ and $p<0.0001$ respectively) (Table 2).

Consequently, we investigated more deeply into factors associated with discordant results. In univariate analysis, BCG vaccination showed a significant association with TST+/IGRA- discordant results, with OR = 2.34 (95%CI, 1.14–4.81), when the other combinations were set as controls [10,11]. In multivariate analysis, when age, working hospital and working